~~Spatiotemporal~~ Improved understanding of regional groundwater drought development ~~of~~ through time series modelling: the 2018-2019 ~~groundwater~~ drought in the Netherlands~~: a data-based approach~~

Esther Brakkee[1], Marjolein H.J. van Huijgevoort[1], Ruud P. Bartholomeus[1, 2]

[1]KWR Water Research Institute, Nieuwegein, 3433 PE, the Netherlands
[2]Wageningen University, Soil Physics and Land Management Group, Wageningen, the Netherlands

Correspondence to: Esther Brakkee (esther.brakkee@kwrwater.nl)

Style Definition: Comment Text

Abstract. The 2018-2019 drought in northwestern and central Europe caused severe damage to a wide range of sectors, and has made clear that even in temperate-climate countries adaptations are needed to cope with increasing future drought frequencies. A crucial component of drought management strategies is to monitor the status of groundwater resources. However, providing up-to-date assessments of regional groundwater drought development remains challenging due to the limited availability of high-quality ~~of available~~ data. This limits many studies to small selections of groundwater monitoring sites, giving an incomplete image of drought dynamics. In this study, a time series modelling-based method for data preparation was developed and applied to map the spatiotemporal development of the 2018-2019 groundwater drought in the southeastern Netherlands, based on a large set of monitoring data. The data preparation method was evaluated for its usefulness and reliability for data validation, simulation and regional groundwater drought ~~quantification and prediction~~assessment. The analysis showed that the 2018-2019 meteorological drought caused extreme groundwater drought throughout the southeastern Netherlands, breaking 30-year records almost everywhere. Drought onset and duration were strongly variable in space, with especially higher elevated areas remaining in severe drought well into 2020. Groundwater drought development appeared to be governed dominantly by the spatial distribution of rainfall and the geological-topographic setting. The time series modelling-based data preparation method was found a useful tool to enable a spatially detailed~~, consistent~~ record of regional groundwater drought development. ~~Applying a~~The automated TSM-based data validation ~~step before analysis turned out to be important for good results~~improved the quality and quantity of useable data, although optimal validation parameters are probably context-dependent. The time series simulations were generally found to be reliable; however, the use of time series simulations rather than direct measurement series can bias drought estimations especially at a local scale, and underestimate spatial variability. ~~Finally, time series modelling showed to be a promising tool for regional-scale drought nowcasting and prediction.~~ Further development of time-series based validation and simulation methods, combined with accessible and consistent monitoring data, will be valuable to enable better groundwater drought monitoring in the future.

1 Introduction

In the summer of 2018, a severe drought hit large parts of ~~northern~~northwestern and ~~western~~central Europe. Extremely low precipitation coincided with high temperatures, both breaking multiple-decade records in many places (see Bakke et al., 2020;

Philip et al., 2020; Toreti et al., 2019)~~.~~. Recurring drought in summer 2019 and early 2020 worsened the situation in large parts of the area. Drying soils and declining water reserves caused damage to agricultural production and natural ecosystems, problems with drinking water and energy production, and widespread forest fires, among other impacts (Bakke et al., 2020; Bastos et al., 2020; Buras et al., 2020; Philip et al., 2020). The kind of 'hot drought' that occurred in 2018-2019 is expected to become more frequent in the future in central and northern Europe (Philip et al., 2020; Toreti et al., 2019).

The Netherlands was one of the countries most hit by ~~the~~these weather extremes (Bakke et al., 2020). The damage was felt mainly in the southern and eastern parts of the country (Van de Velde et al., 2019; Van den Eertwegh et al., 2019; Witte et al., 2020b). In a country traditionally more focused on ~~getting rid of~~discharging water surpluses, the drought of 2018-2019 was felt by many water managers as a wake-up call, sparking a widespread search for solutions to prepare water systems for increasingly frequent drought extremes (De Lenne and Worm, 2020; IenW, 2019; Witte et al., 2020a; Van de Velde et al., 2019). In the southeastern Netherlands, as in many other parts of the world, groundwater is a crucial water source. Accordingly, much of the damage in 2018 was directly related to deep ~~drawdowns~~declines in groundwater levels (LCW, 2020). Among other effects, the groundwater shortages caused severe damage in peatland and brook ecosystems (Witte et al., 2020b) and concerns over the sustainability of increased irrigation and drinking water abstractions (Van de Velde et al., 2019; Van den Eertwegh et al., 2019). Groundwater is often the most persistent water store in the landscape, reacting latest as a meteorological drought propagates into the hydrological system (Van Loon, 2015). This makes proper management of the groundwater a crucial component of drought management strategies.

Previous studies have shown that the response of groundwater to meteorological drought can vary strongly in space. Variations in groundwater response are caused by differences in geology, water management and other catchment characteristics (Bloomfield et al., 2015; Hellwig et al., 2020; Peters et al., 2006; Van Loon and Laaha, 2015). To be able to mitigate and prevent drought damage, it is therefore essential to understand how groundwater drought develops in both time and space. In recent years, water managers in the Netherlands have indeed expressed a need for more up-to-date, locally-specific drought information and predictions to be able to take appropriate measures (IenW, 2019; Pezij et al., 2019; Witte et al., 2020a). ~~Not only the period of meteorological drought itself, but also the recovery of the system after meteorological drought is important to understand.~~

Multiple recent research efforts have aimed at better understanding the variations in groundwater drought and its impacts at national and European scales ~~(Bakke et al., 2020; Bloomfield et al., 2018; Hellwig et al., 2020; Margariti et al., 2019; Van Loon et al., 2017).~~(Bakke et al., 2020; Hellwig et al., 2020; Margariti et al., 2019; Van Loon et al., 2017; Brauns et al., 2020). The 2018(-2019) drought in Europe at larger scales has so far been ~~mainly~~ studied from a meteorological perspective (Bakke et al., 2020; Philip et al., 2020; Toreti et al., 2019)~~. A large-scale analysis of the hydrological drought has recently been made for Scandinavia (Bakke et al., 2020); while for the Netherlands, some assessments of the drought in the groundwater have been done~~ as well as from a hydrological perspective in, among others, Scandinavia and Switzerland (Bakke et al., 2020; Brunner et al., 2019). For the Netherlands, some assessments of the drought in the groundwater have been made based on small numbers of measurement sites and physically-based modelling studies (Van den Eertwegh et al., 2019). What is still lacking, is a more detailed image of how the 2018-2019 drought manifested itself in the groundwater and how this varied in space, based on measurement data. This could provide valuable insights into groundwater drought dynamics and mitigation options in the Netherlands and ~~elsewhere~~similar groundwater-dominated lowland regions.

Groundwater heads are widely monitored in ~~measurement~~observation wells. However, analysis of groundwater drought from these data over large areas is often challenged by data ~~quality.~~quantity or quality (Kumar et al., 2016). Firstly, data usually have to be obtained from multiple organisations and contain errors and other perturbations. Secondly, the length of measured time series is often not sufficient for drought analysis, for which at least 30-year series are recommended (Link et al., 2020). As a result, many~~ data-based~~ groundwater drought studies have focused on relatively few measurement wells with near-natural, long series or on simplified proxies (Bakke et al., 2020; Van Loon et al., 2017; Van den Eertwegh et al., 2019; Kumar et al., 2016)~~; this~~. This may give an incomplete image of the true variability in drought dynamics. In addition, available data usually lags behind the present, hindering the up-to-date drought assessments that water managers need.

To deal with these challenges, several studies have developed methods for automated validation and lengthening of groundwater head time series (Marchant and Bloomfield, 2018; Peterson et al., 2018; von Asmuth et al., 2012). This is usually done with various types of statistical models~~, ranging from regression analysis to artificial intelligence methods~~ (Peterson et al., 2018; Van Loon et al., 2017). One type of statistical modelling that has proven very useful for groundwater data is time series modelling with impulse-response functions (Bakker and Schaars, 2019; von Asmuth et al., 2002). These models describe groundwater head variations at a specific location as a function of driving variables, usually weather data, and a fitted impulse-response function. This type of impulse-response time series modelling (TSM) allows accurate simulations to be made without a need for information on site characteristics. The simulations can be used to identify errors and other atypical behaviour in the data, and to lengthen and harmonise time series, as shown by e.g. Zaadnoordijk et al. (2019), Bartholomeus et al. (2008) and Marchant and Bloomfield (2018). ~~Marchant and Bloomfield~~As such, TSM can enable drought studies to use more observation points and to perform real-time monitoring, without the need for a complex physically-based model. Marchant and Bloomfield (2018) were the first to develop a full time series model-based method to study groundwater drought over a large region in the UK. Although TSM-based analyses appear a valuable tool for groundwater drought assessment, their wider applicability for various cases has not yet been well explored. To be able to widely use TSM data preparation for drought studies, ~~three main~~several questions need to be answered.

Firstly, it is not yet clear what methods are optimal for groundwater data validation. Raw groundwater data sets are usually strongly influenced by errors and disturbances, which can hamper the reliability of analyses such as model calibration and calculation of groundwater characteristics (Post and von Asmuth, 2013; Peterson et al., 2018; Ritzema et al., 2018). Time series modelling can be used to identify time series influenced by disturbances after analysis (e.g. Marchant & Bloomfield, 2018), but also to remove irregularities from the data beforehand. In addition, TSM-based data cleaning can be combined with other more basic consistency checks, improving its effectiveness (Peterson et al., 2018). This validation method has not yet been evaluated ~~specifically~~ for the case of groundwater drought analysis.

Formatted: Font color: Accent 1

Secondly, the reliability of time series simulations for groundwater drought analysis has not been properly tested. To provide lengthened, gap-filled groundwater head series that are suitable for analysis, researchersunderstand the added value of using TSM data preparation, the gain in spatial and temporal cover needs to be balanced with a potential loss of information by cleaning and simulation. Researchers have often used TSM simulations directly as replacement of the data. TheseThis may be justified as these simulations often have a very good fit to the dataobservations (Bakker and Schaars, 2019; Zaadnoordijk et al., 2019); however, this approach inevitably also strips out part of the external influences that are not explicitly included in the model drivers (Peterson et al., 2018; Zaadnoordijk et al., 2019). Drought occurrence and development can be strongly affected by human impacts, as well as by local-scale natural influences such as surface water influence (Margariti et al., 2019; Van den Eertwegh et al., 2019). As such, excluding such external drivers of groundwater levels may provide an incomplete image of drought dynamics (Van Loon et al., 2016). In addition, models may have intrinsic difficulties to correctly represent groundwater behaviour during extreme drought conditions, which may cause deviating soil and groundwater flow processes (Hellwig et al., 2020; Avanzi et al., 2020). This is especially important when time series models are used for 'nowcasting' groundwater observation series. Under extreme drought conditions, this by definition involves modelling system conditions not present in the calibration period and may give incorrect results. It is therefore important to understand how the use of TSM simulations rather than measurement series affects the assessment of drought behaviour.

Finally, the usefulness of TSM for nowcasting and predicting groundwater drought needs to be better understood. Recently, there has been a surging interest in large-scale drought forecasting, which has shown that physically-based groundwater models can predict with some skill up to two months ahead (Honingh et al., 2020; Mackay et al., 2015; Sutanto et al., 2020; Wanders et al., 2019). Time series modelling could provide a very easy alternative to nowcast and predict groundwater drought requiring nothing more than weather data (Bakker and Schaars, 2019; Marchant and Bloomfield, 2018). However, prediction skill may depend on the location and the delay of the groundwater system (Mackay et al., 2015; Marchant and Bloomfield, 2018). Also, models may have difficulties to correctly represent groundwater behaviour during abnormal drought conditions (Hellwig et al., 2020). It is therefore important to better understand how accurate time series models actually are in nowcasting and forecasting groundwater drought.

Given these knowledge gaps, the current study aims to evaluate the usefulness of a time series modelling-based data preparation method for regional analysis of groundwater drought. TheA method will be is developed consisting of data validation, simulation and drought assessment (Sect. 3) and applied to the 2018-2019 groundwater drought in the southeastern Netherlands, to characterise theits development and recovery in time and space (Sect. 4). The usefulness of the 2018-2019 groundwater drought and its recovery. The method will beis evaluated on the usefulness by its performance and reliability with regard to groundwater data validation and simulation; and its added value for series validation and simulation, the effect of simulations on drought assessment, and the potential forthe resulting regional drought prediction.assessment (Sect. 5).

The applied method for data validation and drought assessment, as well as the tests used for its evaluation, are set out in section 2 and 3. The performance of the method and the resulting drought analysis are presented in section 4. In section 5, the resulting

Formatted: Comment Text, Line spacing: 1,5 lines

Formatted: Font color: Accent 1

~~insights into the use of time series modelling-based data methods for groundwater drought studies are discussed, followed by the spatiotemporal drought development of 2018-2019. Final conclusions are given in section 6.~~

2 Study area and data

The study area covers ~~six provinces in~~roughly the southeastern ~~part~~half of the Netherlands (Fig. 1). This is a low-topography area ~~coincides with that part of the Netherlands that lies~~ above sea level ~~and is~~, dominated by Pleistocene ~~era~~ deposits. ~~Most of the~~The study area has mainly sandy sediments at the surface, but ~~part~~ is also partially covered by river clays and loess deposits (Fig. 1b). Elevation is mostly between 0 and 30 m AMSL, with locally higher areas (Fig. 1a). Higher elevations occur in the limestone-loess hill landscape of southern Limburg and on glacier-pushed ridges in Utrecht and Gelderland (areas indicated in Fig. 1a). Land use is dominated by agriculture, while the glacial ridges are covered mainly with forest. The area has a temperate climate with a yearly precipitation surplus~~.~~ (P 700-950 mm j^{-1}, ET_{ref} around 600 mm j^{-1}). In addition, the groundwater system is affected by abstractions for drinking water and irrigation, as well as by drainage systems in the lowest-lying parts of the study area.

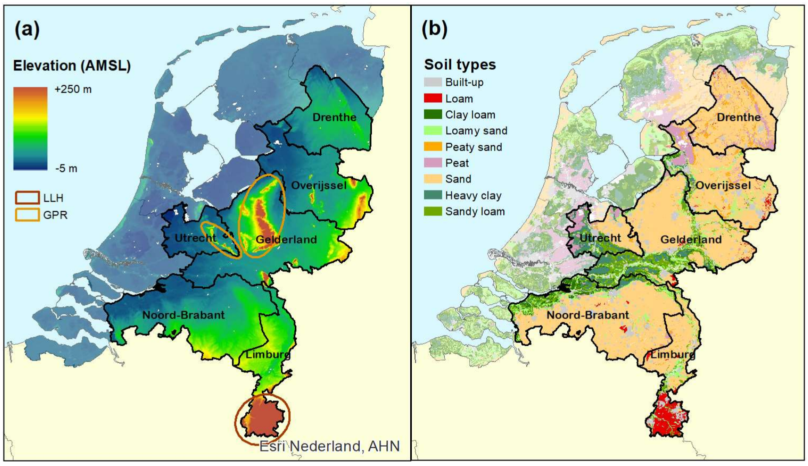

Figure 1: Study area. a: Elevation (AHN, 2019); b: Soil types (WUR, 2006). The higher elevated limestone-loess hill landscape in southern Limburg (LLH) and glacier-pushed sand ridges (GPR) are indicated.

~~**2.2 Input data**~~

Groundwater head data were supplied by several regional water managing bodies. For some areas, additional series were obtained from the Dutch national groundwater database DINO (TNO). The data consist of groundwater head time series with a twice-monthly to sub-daily frequency, mostly running until spring 2019. In addition, metadata of the monitoring wells were available, including location, filter depth and surface level. ~~The different data sets were checked for overlapping wells by well names and coordinates, and overlapping series were combined.~~ Only data from the first filter of boreholes was used, generally representing the phreatic level. ~~Data were cut off at 1 January 1990 and those~~Those series were selected that contained > 10 years of consecutive data to ensure sufficient data for time series model fitting (see Zaadnoordijk et al. (2018)); and ended after 2018-08-31 ~~August 2018~~. The 2018-2019 meteorological drought peaked in summer 2018 (Fig. 3); therefore summer 2018 was chosen as the focus period for model evaluation. This resulted in 2722 series for further analysis.

Daily precipitation (*P*) and reference evapotranspiration (ET_{ref}) were obtained from the Royal Netherlands Meteorological Institute (KNMI) for January 1990 to May 2020 (KNMI, 2020). Data were used from 15 general weather stations (for ET_{ref}) and 114 precipitation stations distributed homogeneously over the study area. Reference evapotranspiration is determined by KNMI following Makkink (1957). The ET_{ref} series did not always cover the full period of interest; gaps were filled with the nearest station that did have full data~~.~~ (maximum distance around 50 km).

Formatted: Font: Italic

Formatted: Font: Italic

Formatted: Font: Italic

3 Methods

The method for data preparation and drought analysis consists of three components (Fig. 2): 1) validation of the observed groundwater heads, 2) simulation of groundwater heads, and 3) conversion to a standardised groundwater index (SGI). ~~The last two steps were also performed for a prediction of the groundwater heads. Finally, each~~Each step ~~was~~is evaluated by one or more tests. In addition, the resulting drought assessment for the case study region is explored as an example of a regional-scale application.

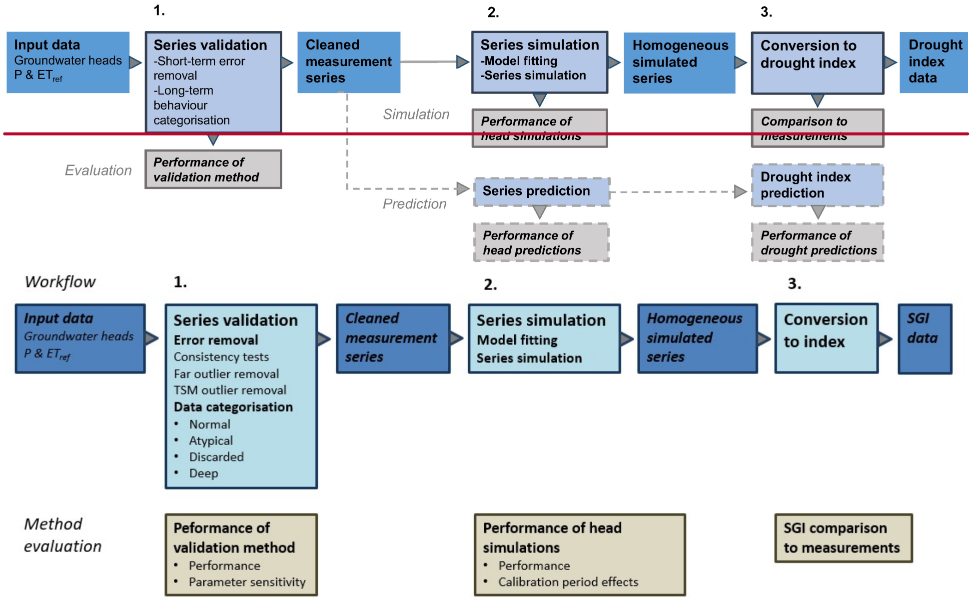

Figure 2: Method workflow.

3.1 Time series modelling method

This study has made use of time series modelling with predefined impulse-response functions, as developed by von Asmuth et al. (2002). Time series modelling was done with the Pastas package for Python developed by Collenteur et al. (2019). The used model setup largely follows Collenteur et al. (2019) and is described in more detail in Appendix A. In short, groundwater levels were simulated as a base level *d*, overlain by a temporal fluctuation in response to external stresses – in this case only recharge. Here, recharge is estimated as:

$$R(t) = P(t) - f \cdot ET_{\mathrm{ref}} \qquad (1)$$

With *f* a calibration parameter. The use of the linear recharge model of Eq. 1 is a simplification that may not be optimal for all locations in this study (Collenteur et al., 2021; Bakker and Schaars, 2019). However, as linear recharge models have been successfully applied in many cases in the Netherlands (e.g. Zaadnoordijk et al., 2019; von Asmuth et al., 2012) and as we aimed to explore the potential of impulse-response time series modelling for drought studies rather than comparing different model setups, we chose to use the simplest model setup possible; see section 5.1.2 for further comments.

The response of groundwater to a recharge impulse is modelled by a scaled gamma function as in von Asmuth et al. (2002) and Collenteur et al. (2019) (see Appendix A). The variation in groundwater heads over time is calculated by convolution of this impulse-response function with the recharge time series.

This gives five parameters to be calibrated for each individual location. Parameter *A* represents the long-term response of the groundwater level to a constant recharge input of one unit, in this case 1 mm; *a* and *n* determine the shape of the recharge response function; *f* is the influence of ET_{ref} relative to precipitation; and *d* is the groundwater base level. For purposes of parameter calibration, also an exponential noise model is fit to the residuals with the additional noise decay parameter *α*.

Table A-1 gives the calibration settings used for each parameter. The default method for parameter optimisation was used, minimising the weighted squared noise using a least squared method (Collenteur et al., 2019).

3.2 Series validation

Data validation in general is a step to check initial data for Raw groundwater data sets are usually strongly influenced by errors and other deviating behaviour. What validation method is suitable dependsdisturbances. Often no information is available on the typepotential sources of deviations in the data and which of them need to be removed for the intended analysis.

, so that these have to be identified from the groundwater data itself (Post and von Asmuth, 2013; Peterson et al., 2018; Ritzema et al., 2018). Phreatic groundwater levels typically follow a yearlyan annual cycle, overlain by faster fluctuations in response to rainfall and evapotranspiration. An actual series of measured groundwater heads will often show deviations from this expected pattern. Deviations may be of short duration, such as caused by a typing error, temporary instrument failure or short-term groundwater abstraction. These can be denoted outliers: a small number of measurements far from the expected level, occurring over a short period (days or weeks) relative to the general (seasonal) fluctuations in most groundwater series (e.g. Peterson et al., 2018). Deviations may also be structural, affecting the series behaviour over months or longer. These are visible as loose outliers; or they may be structural, shown as level shifts, trends and other abnormal patterns in the data series. Both the short (see Appendix A3). Such long-term and structural deviations can result frombe caused by errors, such as instrument drift and typing errors. However, deviations ; however, they can also reflect real groundwater behaviour caused by local natural or human influences, such as rainstorms, floodingsurface water influence or abstraction (Post and von Asmuth, 2013; Zaadnoordijk et al., 2019; Margariti et al., 2019). For one subregion of the study area (Overijssel province, see Fig. 1) log. Log book notes from the data collectors were available; inspection for a small subset of theseour dataset indeed showed that the data were influenced byfrequent disturbances such as short-term extractionsabstractions, changes in water management, sensor problems, relocation of wells, well maintenance and other issues. Also Zaadnoordijk et al. (2019) found that probably a majority of series in Dutch groundwater data sets contain such disturbances.

This kind of groundwater head data clearly require a validation step to become suitableTo prepare the data for the drought analysis, we used a validation setup that treats short-term (outliers) and long-term deviations separately. The validation method aims to remove all important outliers: erroneous outliers will lead to incorrect conclusions on the occurrence of extremes, while real short-term disturbances in the groundwater heads are also less relevant for understanding the slow-developing impacts of drought, which is generally considered to occur on timescales of months to years (van Loon, 2016). Erroneous *long-term* deviations are also undesirable for drought analysis. This step needs to remove the errors, as much as possible; also real but short-term natural and human disturbances inthese disturb the groundwater heads are less relevant for a large-scalelevel distribution on which drought analysis.thresholds are based (see Sect. 3.3). However, the*real* *long-term* deviations in the groundwater level, such as caused by long-term abstraction and land use effects, are important for drought studies and should ideally be retained.

to capture the real variability in drought behaviour (Van Loon et al., 2016). Whether atypical behaviour in a series is caused by errors or by real external influences is very difficult to distinguish by automated methods. Our approach is therefore to filter out all short-term deviations and then classify the series according to their long-term behaviour. The short-term deviations will be denoted as outliers: one or a few measurements lying far from the expected level. The use of categories for long-term behaviour; this allows for retaining some of the potentially influenced series in the analysis, while acknowledging their lower reliability. The validation itself was done by a combination of time series modelling and simple tests, as explained below.

Time series modelling was done with the PASTAS function package for Python. This package has been developed by Collenteur et al. (2019) to allow impulse-response time series models for groundwater heads to be easily applied and combined into larger workflows. Here the most basic settings of PASTAS were used (see Collenteur et al., 2019). Groundwater heads were modelled as a function of measured precipitation and ET_{ref} series, and a gamma-shaped recharge response function. Recharge itself was modelled as a linear combination of precipitation and ET_{ref}. PASTAS also enables nonlinear recharge modelling; we tested the nonlinear model for a subset of series in Brabant, but model fit was improved in only a small minority of series, and so linear recharge modelling was applied for the rest of the study.

DataThe outlier cleaning was done on the original, raw series in severalconsisted of the following steps: (see Table 1 for parameters):

1. Removing measurements Basic metadata consistency check. Measurements below the well filter or > 20 cmTH_{inund} above the surface level; were removed, as these are likely to point to erroneous measurements or metadata.
2. Removing far outliers. The upper and lower 20 % of the by range of. As a series fast first cleaning step, far outliers were identified as potential outliers; if leaving out these measurements reduced theby isolating the top and bottom fraction of the measurement range by more than half, they were classified(F_{range}) and identifying them as outliers and removed.if their removal caused a reduction in range of > TH_{red}.
3. Outlier removal with TSM. A model was fit for each series using precipitation and ET_{ref} from the nearest weather stations and the basic model settings of PASTAS. Fitting was done at a weekly time step to prevent bias towards recent years with more frequent measurements. The simulation interval was calculated as the standard deviation of the residuals, and all measurements outside a range of 4 times this interval around the simulation were removed. This step was repeated a second time to remove smaller outliers.
3. Outlier removal by time series modelling. A model was fit for each series using precipitation and ET_{ref} from the nearest weather stations. All measurements outside a range of n_{sd} times the standard deviation of the residuals around

Formatted: Font: Italic

Formatted: Normal, Don't add space between paragraphs of the same style

Formatted: Font: +Body (Times New Roman)

Formatted: Font: +Body (Times New Roman) the simulation were removed. This step was repeated n_{iter} times to deal with outliers disturbing the model fitting (Peterson et al., 2018; Leunk, 2014).

For the long-term behaviour classification, a new time series model was fittedfit on the resulting cleaned series. The explained variance percentage (EVP, equal to $r^2 \cdot 100$) and model parameters A, f and d were saved. Parameter A represents the long-term response of the groundwater level to a constant recharge input of one unit, in this case 1 mm; f is the influence of ET_{ref} relative to precipitation; and d is the groundwater base level. In addition, a linear trend was fitted through the residual series and the p-value and r^2 of the trend were saved. Finally, the series were checked for consecutive periods with missing data of > 4 years which would hamper the required 10-year data period (Sect. 2) and, if these were present, only the time period after the last such data gap was used. This check had to be done after data cleaning to ensure all data gaps are recognised. Based on these indicators the series were ordered into four categories: of long-term behaviour (see Appendix A3 for examples):

1. Discarded series: series with very strong deviations from the expected behaviour, as indicated by EVP < 60 %, less thanTH_{EVP}; or insufficient data for analysis (< 10 years of data, data gaps of more than≥ 4 years, or no data over June-August 2018;).
2. Deep-groundwater series: mean water table depth (WTD) > 5 m. These series typically showed a very slow, smoothed behaviour and often poor model fit. They were saved as a separate category to reflect their distinct behaviour and potentially less reliable results;; the used validation method is probably less suitable for these series.
3. Atypical series: series with mild deviations: EVP >= 60 %,TH_{EVP}, but containing a trend or atypical parameters. This points to potential errors, external (human) influence or groundwater processes that deviate from the TSM assumptions used in this study. Locations were marked as atypical if they had a trend in the residuals with p< ≤ 0.05 and r^2 >0.15; an f parameter > -0.05 or < -1.95, very close to the parameter bounds > TH_{r2}; or an A parameter > 1.5, far from its normal rangeunusual values for the used dataset. These boundaries were chosen by trial f and error testing on a subset of the series, where they were found to properly separate those series with visually somewhat atypical, but not extremely disturbed behaviour.A parameters (TH_f and TH_A).
4. Normal series: EVP >= 60 %,TH_{EVP}, no other issues.

The cleaned measurement series of the normal, atypical and deep categories were aggregated to a minimum daily time step and saved for further use.daily means and saved for further use. Table 1 shows the validation parameters used for this study. Several parameters were chosen by initial trial-and-error testing; the sensitivity to these parameters was tested as explained below.

The described methodTable 1: Used parameters for data cleaning and categorising was testedthe series validation.

	Parameter		Used value	Justification
Outliers	MetaCheck	Metadata check performed	yes	
	TH_{inund}	Maximum allowed inundation	0.2 m	Shallow inundation possible in study area, deep inundation unlikely (Leunk, 2014)

Formatted: Font: Italic
Formatted: Font: Italic
Formatted: Font: Italic
Formatted: Normal, Don't add space between paragraphs of the same style
Formatted: Font: Italic
Formatted: Font: Italic
Formatted: Font: Italic
Formatted: Font: Italic
Formatted: Font: Italic
Formatted: Font: Italic
Formatted: Font: Not Bold

	F_{range}	Fraction of range identified as potential outlier in far outlier cleaning	0.2	Tested
	TH_{red}	Minimum range reduction (fraction) to remove outliers in far outlier cleaning	0.5	Tested
	n_{sd}	Threshold number of standard deviations to remove outliers	4	Tested
	n_{iter}	Number of iterations in TSM outlier cleaning	2	Tested
Long-term classification	TH_{EVP}	EVP threshold to discard series	60 %	Visually estimated as suitable; see Appendix A2
	TH_{r2}	r^2 threshold of trend in residuals to mark series as atypical	0.15	Tested
	TH_f	Threshold in *f* value to mark series as atypical	> -0.05 or < -1.95	Close to parameter bounds; see Table A1
	TH_A	Threshold in *A* value to mark series as atypical	>1.5	Far from normal range of values for the given dataset; see Table A1

The performance of the validation method was evaluated on a ~~representative subset of the data. Around 120~~test set of 180 randomly selected series (30 from each province). These series were ~~randomly taken spread over the different provinces; from these 56 test series were selected: 44 with visual errors or abnormal behaviour and 12 without. The test series were first~~ visually checked for ~~both short-term outliers and longer-term abnormal patterns. Then the automated~~ the occurrence of 1) outliers (series to clean); 2) serious long-term deviations such as level shifts or strong trends (series to discard); and 3) milder long term-deviations such as lighter trends (series to mark as atypical); see figures A1-4 for examples.

The validation routine was applied to the test set with the standard parameters of Table 1; and with 20 alternative parameter sets (Table A2). In set 2-11, the parameters were varied individually to more conservative (less cleaning and discarding) and more rigorous values (more cleaning and discarding). In set 12-19, combinations of conservative/rigorous outlier cleaning and long-term deviation identification parameters were tested; and in set 20 and 21 versions are tested with only TSM-based outlier cleaning (no basic cleaning step) and no outlier cleaning at all.

The validation results from all parameter sets were compared to ~~this reference. The method was~~ the visual validation and scored ~~for its ability to~~by 1) ~~correctly remove~~correct identification of outliers~~;~~ (cleaned if needed); 2) ~~correctly categorise abnormal longer~~correct identification of serious long-term ~~behaviour; and 3) overall, result in a properly treated (or duly~~ deviations (discarded~~) series. The first two aspects were scored~~ if needed); and 3) correct identification of mild long-term deviations (marked as atypical if needed). Scoring was done as True or False Positive (deviations correctly recognised) and True or False Negative (absence of deviations correctly recognised)~~. The overall performance was scored as *Good* if outliers and patterns were properly cleaned and categorised; *Reasonable* if some errors remained or were over-removed, but without significant influence on the series as a whole; and *Bad* if remaining errors or over-filtering had a significant influence on the character of the series. Groundwater series with mean groundwater depth > 5 m ('Deep') were retained as a separate category as the tested validation method was found unsuitable for these series)~~ for the three categories.

Formatted: Font: Not Bold

3.23 Series simulation

The cleaned series from the validation step were used to simulate groundwater heads for the drought analysis. It is also possiblewas chosen to interpolateuse simulated series, rather than interpolating the original measurement series with TSM (Marchant and Bloomfield, 2018). However, it was chosen to use simulated series, to ensure regular series without sudden level shifts and prevent influence of remaining outliers. First, a PASTASA model was fit on the cleaned measurement series (see section 3.1 and the model parameters were saved. Next, appendix A1); and for those models with an EVP > 60 %, the fitted model parameters and weather data were taken to simulate % (Table 1), a daily-step groundwater heads head series was simulated for the period of interest, in this case 1 January 1990 to 31 May 2020. This setup makes it easy to extend the simulations when new weather data comes available, without re-doing the model fitting procedure. As most measurement series originally ran until spring 2019, roughly one year of 'nowcasting' was added to the data.

The performance of the simulations was assessed by the root mean squared error (RMSE) and the mean error (ME) of the simulated groundwater headslevels over the wholefull length of the measurement series. The mean errorME was calculated as *mean(simulated-observed)* $ME = mean(GWL_{sim} - GWL_{obs})$ to quantify bias. It is possible that theTo assess model performance under dry conditions differs from the overall performance. Thereforespecifically, the measurements of each series were subdivided into 'low-head periods' (measured head < 20th percentile), 'medium-head periods' (20th to 80th percentile) and 'high-head periods' (> 80th percentile), and the RMSE and ME were re-calculated for these periods. Finally, RMSE and ME were determined specifically over July-November 2018, the period in which the meteorological drought was most severe.and hydrological droughts peaked. All performance measures were expressed both as the absolute value in meters, and as fraction of the mean water table depth (WTD) at the location. The latter measure may give a better image of the scale of the errors, as the practical consequences of given errorimpact of a small change in groundwater head areon vegetation and hydrological processes is generally much larger where groundwater levels are normally shallow. (Bartholomeus et al., 2012; Witte et al., 2020b).

The sensitivity of the simulation of drought conditions to the calibration period was also tested. Models were re-calibrated on the period until the start of the 2018 growing season (1 April 2018) and the groundwater behaviour for the rest of 2018 was 'nowcasted' with the available weather data. Simulation performance was again valuated by the RMSE and ME over July-November 2018, and compared with the simulations calibrated on the full period.

The groundwater behaviour at an individual measurement location can be summarised through the recharge response time, which can be derived from the fitted time series models. The response time was here defined as the time after which 50 % of the groundwater head response to a recharge event has occurred (e.g. Zaadnoordijk et al., 2019). It was derived by intersecting the step response function obtained from Pastas (function get_step_response) with the line $0.5A$. These response times are a characteristic of the full groundwater series, not just the drought period. Still, the response times and their spatial distribution give a further indication of the validity of the time series models and the drivers of groundwater drought development.

Formatted: Superscript

Formatted: Superscript

Formatted: Superscript

Formatted: Superscript

Formatted: Font: Not Bold, Font color: Accent 1

3.3 Drought index

To identify drought periods in time series of hydrological variables, and to compare drought severity between locations, standardised drought indices are used. This concept was first developed for precipitation data with the Standardised Precipitation Index (SPI) (McKee et al., 1993). Later, equivalent indices were developed for other hydrological variables. We quantified the development of meteorological drought over 2018-2020 by the three-month-aggregated Standardised Precipitation Evaporation Index (SPEI) (Vicente-Serrano et al., 2010). The study area was divided into four zones (west, north, mid-east, southeastsee Fig. 2); the SPEI-3 for each zone was calculated from the average precipitation of all weather stations within the zone and the distance-weighted mean reference evapotranspiration of the three stations closest to the midpointET_{ref} of the three stations closest to the midpoint. This midpoint method was necessary to obtain representative values for each zone from the relatively few evapotranspiration stations present (15). SPEI was calculated by a normal distribution transformation for simplicity; the three-month accumulation time was chosen because this most clearly showed the meteorological droughts at a time scale comparable to the variations in groundwater level.

For groundwater heads the Standardised Groundwater Index (SGI) was developedapplied (Bloomfield and Marchant, 2013). To calculate the index values, the The SGI method consists of transforming a measured groundwater headshead series at a specific location are transformed to a standard normal distribution. This gives; this produces a drought index series varying roughly between -3 and 3, indicating conditions from extremely dry to extremely wet compared to the normal situation at the specific location.. When analysing drought indices for multiple locations, a common reference period must be used;. It is generally recommended to beuse a period of at least 30 years. to ensure a proper estimation of the long-term "normal situation" (McKee et al., 1993; Van Loon et al., 2016; Ritzema et al., 2018). Here, the period January 1990 - December 2019 is used throughout as the reference period.

For precipitation, the transformation step is usually done by fitting a gamma distribution function to the data (McKee et al., 1993). . For groundwater heads, however, distribution shapes vary widely between locations (Bloomfield and Marchant, 2013; Dawley et al., 2019; Loáiciga, 2015). It is possible to fit individual parametric distribution functions to the groundwater series, but the 30-year monthly series used here are probably insufficient to do this reliably (Link et al., 2020), givingFitting individual parametric distribution functions to each location based on the 30-year monthly series used here is likely to give unreliable results; for example, Link et al. (2020) find that in most cases more than 100 data points are needed for fitting reliable parametric distributions on hydrological series, while incorrect transformations give a high risk of biased drought index values (Svensson et al., 2017). Groundwater levels were therefore transformed using a normal scores transform (see e.g. Bloomfield and Marchant, 2013). This is a nonparametric transformation method that has the advantage of being simple and transparent and circumvents the risk of bias due to erroneous distribution fits. For each location, the simulated series was first aggregated to a monthly time stepmean levels. Transformation was then done separately for each calendar month. For each calendar month with n years of data, in this case 30, cumulative probability values are taken, uniformly spaced over the interval $(1/n2n)$ to $(1-1/n2n)$; the corresponding SGI values are found by applying an inverse cumulative distribution function to these values.

The resulting SGI values are assigned to the groundwater head measurements of the given calendar month by their rank from low to high. This method of calculating SGIs results in a limited number of 'discrete' SGI values that ~~have a relatively weak relation with occurrence probability, but~~ correspond directly to the rank of the groundwater level compared to the rest of the reference period. Table ~~1~~2 gives the SGI values and their corresponding rank and drought severity in this study. The drought severity classes follow the classification by McKee et al. (1993) that has been frequently used in drought studies. Note that the SGI, unlike the SPI, is not aggregated over multiple months; the SGI values given here therefore represent 'SGI-1'.

Table 2: Used categories for the standardised groundwater index, with the corresponding groundwater level rank in a 30-year record.

SGI	Drought category	Rank (dry → wet)
> 0	No drought	>15 *(wettest 15 years)*
0 to **-1**	Mild drought	6 ~~-~~– 15
-1.5 to **-1**	Moderate drought	3 ~~-~~– 5
-2 to **-1.5**	Severe drought	2
< **-2**	Extreme drought	1 *(~~dryest~~driest year)*

The SGI values for the months outside the reference period (January 2020 – May 2020) were estimated by linearly interpolating the groundwater head-SGI relation for the calendar month. If the heads fell outside the range reached in the reference period, they were assigned the most extreme SGI value.

To test how the use of TSM simulations rather than measurement series affects drought analysis, SGI values were also calculated directly for a selection of locations that had long measurement series. ~~From the cleaned measurement series of the validation step, those were selected that started before 1 January 1993~~To collect enough series for comparison while preventing the influence of differing time periods, a minimum of 27 years was used. All series with at least 27 years of data (starting before 1 January 1993) were selected from the cleaned measurement series, resulting in 531 series. The SGI values for 2018 were calculated in the same way as for the simulated series, with the SGI of a calendar month calculated only if at least 25 years of data were available. In some cases the number of data points will thus be some smaller than for the simulation-based SGI. However, an *n* of 25 instead of 30 does not affect the classification for the lowest drought categories as shown in Table 2; also an exploratory test (not shown) indicated that the slight mismatch in period did not affect the patterns in the resulting comparison. The simulation-based and measurement-based SGI values were compared by regression~~.~~ (Spearman's ρ).

Formatted: Font: Not Bold

~~**3.4 Drought prediction**~~

~~Finally an estimate was made of the drought *prediction* performance of the time series models. If weather predictions are available, time series simulations can be easily extended into the future. However, as the predicted period is not included in the calibration, the quality of the predictions is likely to be lower than for the normal 'fully calibrated' simulations. This is especially important for the prediction of extreme drought, which by definition involves system conditions not present in the~~

calibration period. To test the performance of the time series models for predicting extreme drought conditions, models were re-calibrated until the start of the 2018 growing season (1 April 2018); and the groundwater behaviour for the rest of 2018 was 'predicted' with the available weather data. As such, an 'upper limit' of the prediction performance is estimated, representing how well the 2018 drought would have been predicted had perfect weather predictions been available. The prediction error in groundwater levels was quantified by the RMSE and mean error ME over July-November 2018.

Previous studies have found that in slow-reacting groundwater systems and dry situations, initial conditions can control the quality of model predictions many months forward, irrespective of weather forecasts (Honingh et al., 2020; Mackay et al., 2015; Sutanto et al., 2020). The type of time series models used here rely only on transforming of a time series of recharge to deviations in groundwater heads. The predicted heads are therefore insensitive to the initial conditions simulated at the start of the prediction period. For forecasting, it might be advantageous to include the true initial condition into the preditctions. The effect of a simulation residual on subsequent simulated values be estimated as:

$$RE(t) = R_{ini} * e^{\wedge}(-t/\alpha) \quad (1)$$

Where $RE(t)$ is the remaining effect of the residual at time t after the start of predictions, R_{ini} is the residual at the start of the prediction period, and α is the decay parameter of the noise model (eq. 7 in Collenteur et al., 2019). Adding the series of residual effects to the predicted values thus draws these towards the real values, with the effect decreasing over time.

To estimate how the prediction error in groundwater heads would propagate to the drought quantification, SGI values were calculated both for the predicted series and for the same series with the prediction period replaced by the measurement data. The performance of the SGI predictions was quantified by the mean and maximum absolute error of the prediction- versus the measurement-based SGI values. As such, the difference between the prediction-based and measurement-based SGI values gives an indication of the performance in predicting the occurrence of drought.

4 Results

Here, we present the outcomes of the drought analysis and the evaluation of the time series modelling-based data preparation method. We first show the performance of the method for validation and simulation of groundwater head series; then we present the analysis of the 2018-2019 groundwater drought. Finally, the performance of the TSM method for drought quantification and prediction is shown.

4.1 Performance of TSM data preparation for groundwater head series

The performance of the applied validation method, based on a combination of basic tests and TSM, was tested on a subset of the groundwater series. The method generally identified longer-term irregularities in behaviour well (Table 2, middle columns). More frequently, it incompletely removed outliers or detected outliers that were visually not clearly erroneous (left columns). Overall, the validation method was successful for a majority of the test series (68 %, right columns). For part of the series (20 %), validation was classified as reasonable, with some errors remaining or slight over-smoothing, but without a substantial

~~effect on the overall series, thus being unlikely to affect drought analysis. For a small fraction of the test series (5 %), validation was unsuccessful and more important irregularities remained. Thus, a small number of potentially erroneous series is likely to remain in the data used for the drought analysis.~~

~~Table~~ 4.1 Usefulness of TSM method for drought data validation and simulation

4.1.1 Validation performance

The validation performance for the standard validation parameter set is shown in Table 3. For a large majority of test series the routine performed a correct action with regard to cleaning outliers, discarding strongly deviating series and marking atypical series. In the outlier cleaning, there is a relatively large fraction of false positives (removal of non-existing outliers). This mainly occurs for points in well-modelled series, without affecting the character of the series or the drought extremes. The false negatives (outliers not recognised) partly did concern influential outliers; another relatively frequent problem was the incomplete removal of a group of outliers (not shown in Table 3). With regard to the strong long-term deviations, there is a relatively large fraction of false positives (unduly discarded series). This is partly caused by the incomplete outlier cleaning for some of the series. The number of series marked as atypical by both the visual and automated validation is relatively small. This category is hard to identify consistently by visual inspection, which may explain the false positives and negatives.

Table 3~~: Outcomes of the validation method test: performance of the method in cleaning of outliers, long-term patterns, and the series as a whole. Given is the number of test series in each performance category; see 3.1 for a description of the test.~~
: Validation performance for the standard parameter set (Table 1). Number of series with insufficient data is 19, so n_{total}=161. True Positive=identified in both manual and automatic validation; True Negative=not identified in either manual or automatic validation; False Positive=identified in automatic validation but not in manual validation; False Negative=identified in manual but not in automated validation. Excl. deep: excluding deep-GWL series. Last column: percentage of series with outliers and long-term deviations correctly or reasonably identified.

Outliers	~~Pattern~~True Positive	~~Whole series~~True Negative	False Positive	False Negative	False Negative excl. deep	Correct clean action
~~Performance~~	~~No. series~~71 (44%)	~~Performance~~ 56 (35%)	~~No. series~~26 (16%)	~~Performance~~ 8 (5%)	~~No. series~~6 (4%)	79 %
~~TP~~Strong long-term deviations	~~16~~True Positive	~~TP~~True Negative	~~20~~False Positive	~~Good~~False Negative	~~38~~False Positive excl. deep	Correct discard action
~~TN~~	~~12~~32 (20%)	~~TN~~103 (64%)	~~23~~26 (16%)	~~Reasonable~~0 (0%)	~~11~~22 (14%)	84 %
~~FP~~Mild long-term deviations	~~13~~True Positive	~~FP~~True Negative	~~8~~False Positive	~~Bad~~False Negative	~~3~~False Positive excl. deep	Correct mark action
~~FN~~	~~15~~7 (4%)	~~FN~~131 (81%)	~~5~~11 (7%)	~~Deep~~12 (7%)	7 (4%)	86 %

The parameter sensitivity test (see Table 4 and Appendix A2) showed that the standard parameter set performed relatively well in comparison with other parameter sets. The sensitivity to the parameters of the far outlier cleaning (F_{range}, TH_{red}) and the number of iterations in the TSM outlier cleaning (n_{iter}) was low, while the standard deviation range for the TSM cleaning (n_{SD}) and the thresholds for discarding and marking series (TH_{EVP} and TH_{r2}) did have a large effect. Applying an outlier cleaning

Inserted Cells ... [7]
Merged Cells ... [1]
Inserted Cells ... [10]
Inserted Cells ... [8]
Formatted ... [2]
Inserted Cells ... [9]
Formatted ... [3]
Formatted Table ... [4]
Formatted ... [5]
Formatted ... [6]
Formatted ... [11]
Formatted ... [12]
Formatted ... [13]
Formatted ... [14]
Formatted ... [15]
Formatted ... [16]
Formatted ... [17]
Formatted ... [18]
Formatted ... [19]
Formatted ... [20]
Formatted ... [21]
Formatted ... [22]
Formatted ... [23]
Formatted ... [24]
Formatted ... [25]
Formatted ... [26]
Formatted ... [27]
Formatted ... [28]
Formatted ... [29]
Formatted ... [31]
Formatted ... [30]
Formatted ... [32]
Formatted ... [36]
Formatted ... [33]
Formatted ... [34]
Formatted ... [35]
Formatted ... [37]
Formatted ... [38]
Formatted ... [39]
Formatted ... [40]
Formatted ... [41]
Formatted ... [42]
Formatted ... [43]
Formatted ... [44]
Formatted ... [45]
Formatted ... [46]

step in general increased the simulation performance (mean EVP 60 to 62 %, set 1 vs 21) and allowed more series to be retained for analysis (60 % to 64 % of series), with the TSM cleaning being responsible for most of the outlier cleaning. Taking a conservative low EVP threshold appears to give a good performance on the strong deviation identification (set 8 and 16), but the number of false negatives is high, while a strict EVP threshold of 80 % causes a majority of series to be discarded. Changing the threshold on the residual trend to mark series as atypical (set 10 and 11) caused either almost all or almost no series to be marked and did not substantially improve the performance.

Table 4: Summary results of validation parameter sensitivity test. Nr Discard/Atypical: number of series discarded/marked as atypical. Cleaning/Discard/Marking correct %: percentage of series with correct action identified for cleaning, discarding and marking. See Table A1 for explanation of the parameter sets.

Set	Name	Mean EVP [%]	Nr Discard	Nr Atypical	Cleaning correct %	Discard correct %	Marking correct %
1	*Standard*	*61.9*	*58*	*18*	*79*	*84*	*86*
2	FarOutliersConservative	62	58	18	80	84	86
3	FarOutliersRigorous	61.9	58	18	79	84	86
4	OutliersConservative	60.6	64	17	80	81	86
5	OutliersRigorous	68.8	41	28	60	86	82
6	IterationsConservative	61.7	61	18	79	82	86
7	IterationsRigorous	62.2	58	18	79	84	86
8	EVPConservative	61.9	29	33	79	86	80
9	EVPRigorous	61.9	119	4	79	47	88
10	TrendConservative	61.9	58	7	79	84	88
11	TrendRigorous	61.9	58	39	79	84	74
12	OutliersConservative_EVPConservative	60.5	29	30	80	86	82
13	OutliersConservative_EVPRigorous	60.5	122	4	80	45	88
14	OutliersConservative_TrendConservative	60.5	66	7	80	80	88
15	OutliersConservative_TrendRigorous	60.5	66	36	80	80	75
16	OutliersRigorous_EVPConservative	71.1	15	45	59	89	75
17	OutliersRigorous_EVPRigorous	71.1	82	8	59	68	87
18	OutliersRigorous_TrendConservative	71.1	36	13	59	87	85
19	OutliersRigorous_TrendRigorous	71.1	36	45	59	87	72
20	Standard_TSMcleaningOnly	62.1	57	19	79	84	86
21	Standard_NoOutlierCleaning	59.9	64	16	68	81	88

When applied to the full study dataset, the validation procedure discarded 31 % of the groundwater head measurement series, so that 1869 of the original 2722 series remained for analysis. A poor model fit was the most frequent cause for discarding. 10 % of the series were maintained as atypical series, while another 12 % of locations had a deep groundwater table, being less suitable for the used validation method.

4.1.2 Simulation performance

In the simulation step, 1632 locations were modelled with sufficient quality (EVP > 60 %). Overall, these series were simulated with an average error of 14 cm, resulting on average in a 20 % error in the groundwater table depth (Table 35). The bias is low with -1 mm. Subdivision into dry, normal and wet conditions (0-20th, 20-80th and 80-100th percentile of groundwater levels, respectively) shows that the errors are larger for more extreme groundwater levels. (dry and wet conditions). More precisely, the models tend to underestimate the extremes: there is a positive average bias in periods of low groundwater levels, and a negative bias when groundwater levels are in their high ranges. There was no clear spatial pattern in this bias. Also during the main period of groundwater drought in July-November 2018, the simulation error is above average with 18 cm, but there is only a small negative bias of 1 cm.

Table 35: Performance of the groundwater head simulations for the full simulation period and summer 2018. RMSE=Root Mean Squared Error, ME=Mean Error of simulations versus measurements, given in meters and as fraction of the mean groundwater table depth (WTD).

	RMSE		ME (mod-obs)	
	Mean value *(range)* [m]	Fraction WTD [-]	Mean value *(range)* [m]	Fraction WTD [-]
Full period	0.14 *(0.03…1.7)*	0.20	-1.2·10^{-3} *(-0.3…0.2)*	8.1·10^{-3}
Dry (0 – 20p)	0.16 *(0.03…2.0)*	0.25	0.076 *(-0.7…0.6)*	0.15
Normal (20 – 80p)	0.12 *(0.02…1.6)*	0.18	-3.3·10^{-3} *(-0.3…0.4)*	0.039
Wet (80 – 100p)	0.15 *(0.03…1.7)*	0.20	-0.070 *(-1.3…0.3)*	0.089
Jul-Nov 2018	0.18 *(6.0·10^{-3}…3.2)*	0.29	-0.010 *(-2.9…1.5)*	0.22
Jul-Nov 2018, calibrated until 1 April 2018	0.20 *(1.0·10^{-3}…3.7)*	0.31	-0.015 *(-3.5…1.2)*	0.24

Formatted Table

Formatted Table

Formatted: English (United Kingdom)

Formatted: English (United Kingdom)

4.1.3 Calibration period sensitivity

In addition to the fully calibrated simulations, the sensitivity of the model simulations during drought to the used calibration period was tested (Table 5, last row). When the 2018 drought summer was simulated with a TSM model calibrated until spring 2018, the average error in the predicted groundwater heads was 20 cm, giving a relative error in the groundwater depth of 31 %, thus performing slightly poorer than the fully calibrated simulations (error of 20 %). Similar to the fully calibrated simulations, there is a (small) negative mean error, indicating that the declines in groundwater level over summer, and thus the severity of drought, are slightly overestimated. This means that, as expected, the simulation of groundwater levels under extreme drought conditions outside the range of conditions in the model calibration has a relatively low reliability. However, the difference in average error is only 0.03 m, indicating that the effect is relatively small compared to the error already present in the fully calibrated simulations. There are no clear spatial patterns in the RMSE of the simulations (not shown). The sensitivity to the calibration period thus appears independent of specific catchment characteristics in the study area.

4.2 Development and recovery of the 2018-2019 groundwater drought in the Netherlands

The groundwater drought of 2018-2019 was driven by exceptionally dry weather conditions. The meteorological drought started in spring 2018 and peaked in late summer (Fig. 3). After a relatively normal winter, summer 2019 again showed moderate to severe drought. The winter of 2019-2020 was relatively wet, but exceptionally low rainfall in spring 2020 caused a return to extreme meteorological drought conditions. The meteorological drought was not spatially uniform. Especially in spring 2018 and summer 2019, the western part of the study area experienced less dry conditions than the east (Fig. 3).

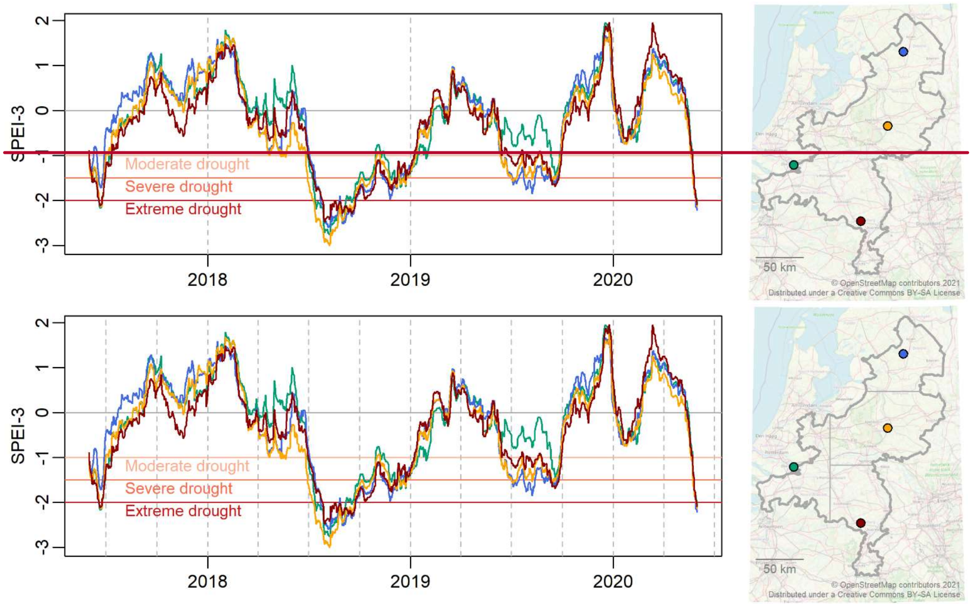

Figure 3: Development of the meteorological drought over 2018-2020 in the west, north, mid-east and southeast sections of the study area given by the 3-month SPEI. The map shows the ~~midpoints of the~~ four sections.

The development of the groundwater drought in the southeastern Netherlands over 2018 is visualised in Figures 4 and 5. The 2018 growing season started with uniformly normal to high groundwater levels over the study area (Fig. 4). Drought started developing in May and June, with drought onset varying between locations. By July and August, severe to extreme groundwater drought occurred over most of the area. In September, heavy rain in ~~part~~the west of the study area slightly alleviated the drought conditions. However, the drought situation worsened again in autumn, reaching its height in October and November when the simulations show almost uniform extreme drought over the study area. By December, a slow recovery is visible.

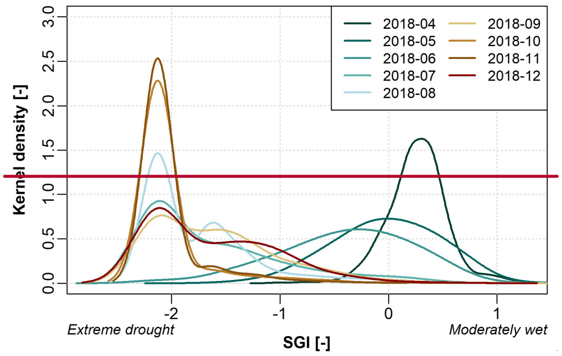

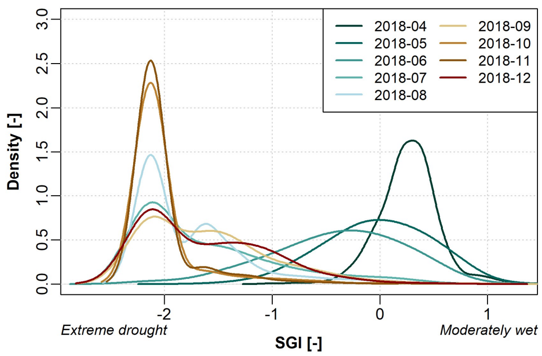

Figure 4: Monthly distributions of the Standardised Groundwater Index over 2018 in the southeastern Netherlands.

The simulated data show distinct spatial patterns in the development of the groundwater drought (Fig. 5). Especially southern Limburg and the ridges in Utrecht and Gelderland with their distinct geology and topography (see Fig. 1) reacted more slowly than the rest of the study area and did not experience drought conditions yet in 2018. Also the fast recovery of the low-lying western Utrecht area in autumn stands out.

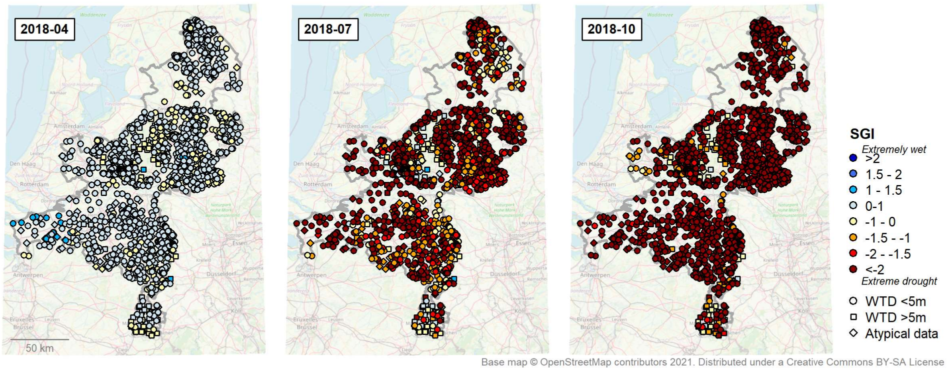

Figure 5: Groundwater drought development in 2018: SGI of simulated series. WTD: Water table depth.

The simulations over 2019-2020 show that also drought recovery was strongly variable in space (Fig. 6). In spring 2019, groundwater heads in the west of the study area were again approaching normal levels, but the eastern regions had recovered poorly. By this time extreme groundwater drought had also developed on the high ridges and in southern Limburg. The summer of 2019 again brought severe to extreme groundwater drought, this time clearly concentrated in the east of the study area, corresponding to the differences in meteorological drought. In March 2020, groundwater levels had returned to relatively high levels. However, the exceptionally dry weather in April rapidly resulted in a new severe drought situation by May.

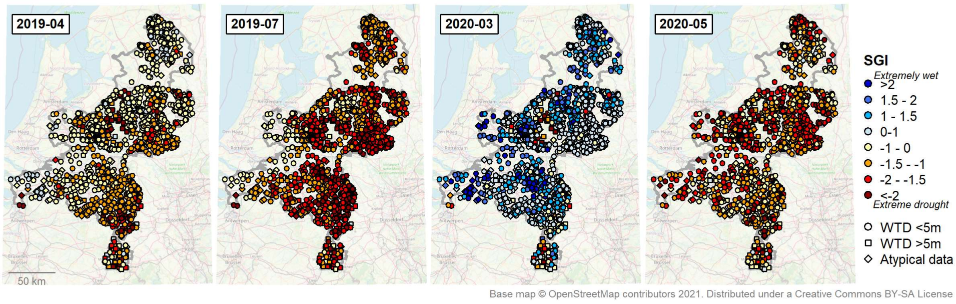

Figure 6: Groundwater drought over 2019-2020: SGI of extended groundwater series. WTD: Water table depth.

~~To further explore the spatial variations in drought behaviour, the~~ The groundwater response ~~time was mapped for all monitoring locations (Fig. 7). The response time, the time after which 50 % of the groundwater head response to a recharge event has occurred, can be obtained directly~~times derived from the ~~parameters of the fitted~~ time series ~~model for a specific location.~~models are shown in Fig. 7. The ~~found~~ response times ~~ranged~~range from a few days to up to two years, but ~~were~~are generally relatively short: 94 % of locations ~~had~~has a response time of less than one year. The spatial distribution of the response time corresponds with the topography and the occurrence of glacial sand ridges in the landscape (Fig. 1) and with the propagation speed of meteorological drought to groundwater drought in 2018-2020 (Fig. 5, 6).

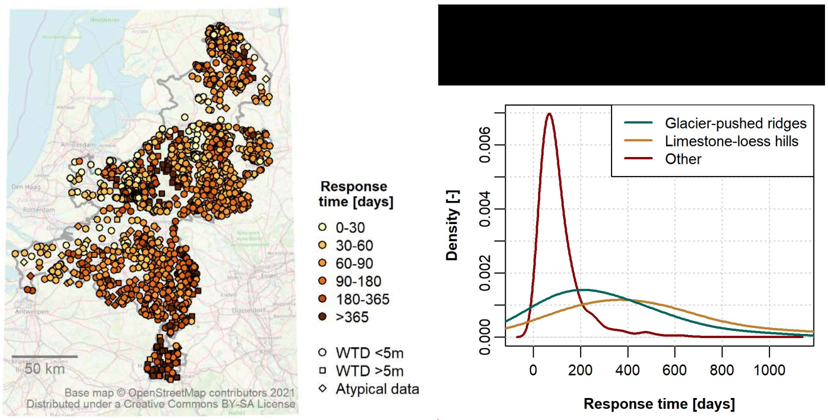

Figure 7: Response time to recharge as derived from the fitted response functions. <u>**See Fig. 1 for the location of subregions.**</u>

4.3 Usefulness of TSM method for <u>regional</u> drought ~~quantification and prediction~~<u>assessment</u>

For a subset of the locations (n = 531), a long groundwater measurement series was available and the SGI values resulting from the simulated series could be compared to those obtained directly from the cleaned measurement series (Fig. 8). The comparison shows that the simulations follow the same general drought behaviour as the measurement series, as the two follow a 1:1 line (Spearman's ρ = 0.8). However, the simulations generally show a smaller spatial variation than the measurements. This is also visible in measurement-based SGI maps (Fig. 9), which show more scatter and local extremes than the simulation-based drought maps. In addition, the simulations for 2018 tend to slightly overestimate drought severity in the low ends of the drought (lower left in Fig. 8). This is contrary to the general tendency of the head simulations towards positive bias during drought periods, shown in Table ~~3~~<u>5</u>.

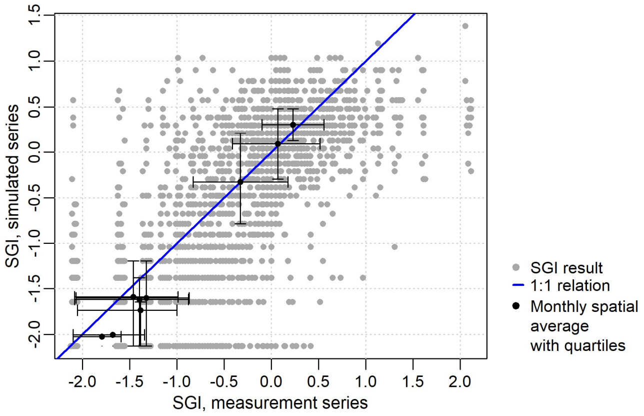

540 **Figure 8: Comparison of SGI values over April-December 2018 based on cleaned long measurement series (x axis) and based on simulated series (y axis) for all location-month combinations (grey dots). Black dots show the average over all locations for each month, with quartiles (spatial variation).**

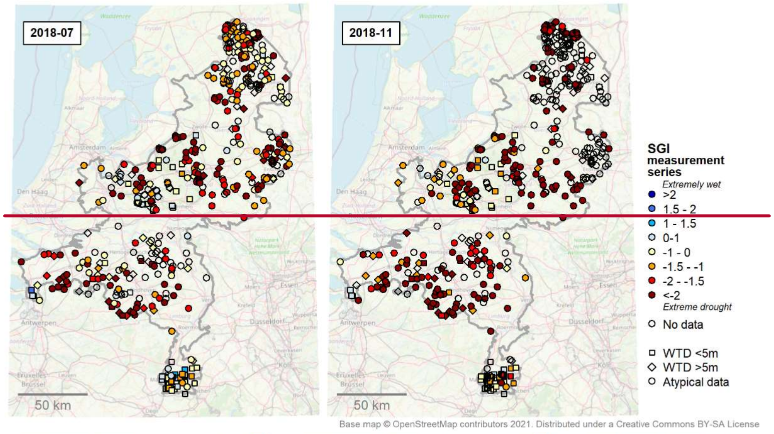

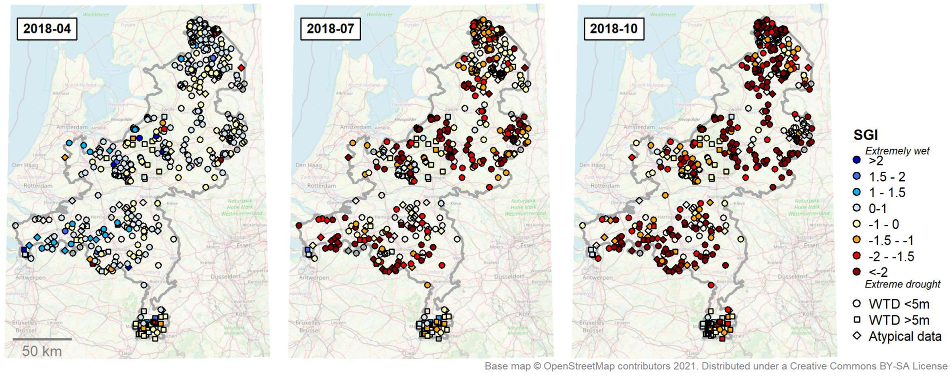

Figure 9: SGI for ~~two~~three months in 2018 based directly on cleaned long measurement series. ~~'No Data'~~Empty symbols indicate insufficient data to enable drought index quantification.

~~In addition to the simulations, it was also tested how well the time series models, calibrated until the start of the growing season, would have predicted the 2018 groundwater drought from weather data only (Table 4). The average error in the predicted groundwater heads was 20 cm, giving a relative error in the groundwater depth of 31 %. The (small) negative mean error indicates that the declines in groundwater level over summer, and thus the severity of drought, are slightly overestimated. This pattern is also visible in the simulations themselves. The prediction performance is poorer than that of the normal simulations with all data included in the calibration (Table 3). This means that, as expected, the prediction of groundwater levels under extreme drought conditions has a relatively high unreliability. However, the difference in average error is only 3 cm, indicating that the effect is relatively small compared to the error already present in the fully calibrated simulations.~~

~~The prediction errors in the groundwater head were estimated to result in an average absolute SGI error of 0.34. With the used methods for SGI calculation and n=30 years, an error of 0.48 is required to cause a shift between "extreme drought" and "severe drought", and an error of 0.26 will cause a shift between severe and moderate drought. This means that most locations that were in extreme drought in summer-autumn 2018 were also predicted as such, despite errors in the heads themselves. However, there is a large variation between locations in the size and direction of the drought index errors. Predictions are good for many locations (error ≈ 0), while some are classified at the complete other side of the drought spectrum than the measurements (error of -2.9; see Table 1).~~

~~**Table 4: Performance of the drought predictions for summer 2018: means and ranges of performance measures over all model locations. RMSE=Root Mean Squared Error, ME= mean error, MAE=mean absolute error.**~~

~~**Prediction of groundwater heads, summer 2018**~~			~~**Prediction of SGI, summer 2018**~~
-	~~**Mean value *(range)* [m]**~~	~~**Mean fraction of WTD [-]**~~	~~**Mean value *(range)* [-]**~~
~~**RMSE**~~	~~0.20 *(1·10⁻³...3.7)*~~	~~0.31~~	-
~~**ME**~~	~~-0.015 *(-3.5...1.2)*~~	~~0.24~~	~~-0.21 *(-2.9...1.0)*~~
~~**Error minimum head**~~	~~-0.048 *(-4.9...1.5)*~~	~~0.34~~	-
~~**MAE**~~	-		~~0.34 *(0.0...2.9)*~~
~~**Maximum AE**~~	-		~~0.72 *(0.0...3.5)*~~

~~There are no clear spatial patterns in the RMSE of the predictions, nor in the estimated error in SGI (not shown). The prediction error in the minimum level is also largely randomly distributed, although some larger overestimations occur in part of southern Noord-Brabant, while the minimum levels are underestimated in southern Limburg. The performance of the predictions thus appears independent of specific catchment characteristics.~~

~~The initial conditions simulated at the start of the growing season had an average absolute error of 15 cm. Including the true initial groundwater heads on March 31 into the predictions led to small improvements in the prediction on a short term: this reduced the prediction errors after 1 and 7 days on average by 14 cm and 5 cm, respectively. However, after a month or more the effect of the initial residual becomes insignificant, and after 4 months, the inclusion of initial conditions leads to an average increase in error of 0.9 cm. Inclusion of the residual at the start of the growing season therefore did not improve drought predictions in the height of summer.~~

5 Discussion

5.1 Usefulness of TSM data preparation for drought analysis

The performed study aimed to evaluate the usefulness of time series modelling-based data processing methods for groundwater drought studies. The application of ~~the~~a TSM-based method to the 2018-2019 drought in the Netherlands has provided ~~several~~ new insights into how TSM methods can be used for data validation~~;~~, how reliable they are for the quantification of extreme groundwater drought situations;, and their usefulness forhow they can contribute to regional groundwater drought predictionassessments.

Formatted: Font color: Accent 1

5.1.1 Validation methods for groundwater data

A validation method was applied that combines basic error tests with time series modelling-based identification of irregularities, while separately treating short-term outliers and long-term atypical behaviour. It separately. Pre-analysis outlier cleaning was found thatto improve the data availableuseability of series for this study, and this may be true for many cases, contained large numbers of outliers with various sources. Removing these outliers often led to a good TSM fit that was not possible before this procedure. Therefore, with the kindTSM simulations as well as the identification of data used in this study, pre-analysis outlierlong-term series behaviour. Outlier cleaning is therefore likely to improve results compared to performing a more limited validation, or identifying impacted series only after simulation. The validation method performed reasonably with regard to outlier removal, but not optimally (Table 2). The outlier cleaning may be further improved by using more iterations (e.g. Peterson et al., 2018), although care must be taken to avoid over-smoothing3, Table A3). The time-series based outlier cleaning appeared more effective in comparison to basic cleaning methods, although the latter can be valuable as a computationally cheap cleaning step for large data sets.

The TSM-based validation also provedappeared suitable for identifying long-term atypical behaviour in the head measurement series. However, the thresholds for separating series in different reliability classes (here 'discard' and 'atypical') are likely to be dependent on the data used and the aim of the study, and are difficult to set objectively. The current study aimed to provide a spatially detailed regional drought assessment, covering the range of site conditions; this requires retaining as many series as possible, while removing the most unreliable and disturbed series and identifying series with milder potentially unreliable behaviour. The chosen parameters were found reasonable to reach this separation (see Fig. A5, A6) but setting objective parameter values would require comparison with a large data set with detailed information on the sources of variations and errors, which was not available in this study.

In this study, we could not explicitly separate erroneous and real atypical patterns in this study. Many of the long-term non-weather influences on the groundwater, such as structural abstractions and land use, are likely to be included implicitly in the simulations, as the time series models will model any external influence that correlates with weather or modifies the recharge response. In addition, the use of a classification for long-term behaviour allowed for retaining moderately 'atypical series' rather than filtering out all impacted locations. Still, the validation is likely to retain some series with erroneous patterns and discard some real behaviour.

The separation of errors could be improved by including additional driving factors in the time series modelling, such as surface water fluctuations (Bakker and Schaars, 2019; Van Loon et al., 2016; Zaadnoordijk et al., 2019); however, this requires substantially more data and modelling effort. Another potential approach is to make use of the spatial coherence of groundwater behaviour to separate errors. For example, Lehr and Lischeid (2020) and Marchant and Bloomfield (2018) used the spatial coherence of observed groundwater patterns as an indication of their reliability, and to relate clusters of similar series to some external (human) impact. It would be valuable to explore such extensions of TSM to improve validation methods for groundwater drought analysis. This will allow for a better understanding of the different natural ánd human drivers of drought development.

Although the validation-simulation method generally performed well for the given data, it was less suitable for locations with ~~very~~ deep groundwater tables~~,~~ (here > 5 m), dominated by multi-year head fluctuations. Here, model fit was often low, leading to poor outlier identification and models being discarded for a large proportion of these locations~~.~~ (66 % discarded vs 27 % for shallower locations). This issue was also found by Marchant and Bloomfield (2018) and Zaadnoordijk et al. (2019) for locations with thick unsaturated zones. To enable TSM simulation in such cases, measurement series are needed that are substantially longer than the minimum of 10 years used here to include several response cycles of the groundwater system.

5.1.2 Reliability of TSM groundwater level simulations during extreme drought

It was found that impulse-response function-based time series models on a general level produced reliable groundwater head simulations. They described most of the groundwater head series very closely, with a low overall bias (Table 5). The comparison of simulation- and measurement-based SGI values (Fig. 8) showed a good correlation (Spearman's ρ = 0.8). ~~3). However, the time series models tended to underestimate extreme conditions somewhat, including dry summer conditions, although the simulations for summer 2018 interestingly had a small negative bias in the lowest ranges. The~~Also, as discussed further below, the general patterns shown by the drought index maps match well with the experience of water managers during the 2018-2019 drought.

However, the model simulations also showed important deviations, especially at local scales and during the most severe drought periods. The simulation RMSE and mean errors amounted locally to high levels (Table 5), especially during more extreme conditions. Also expressed as fraction of the WTD large errors occurred (Table 5). This means that application of the current TSM method could lead to misinterpretations of drought impacts at local scales, for example on the survival of marsh vegetation or groundwater-dependent streams (Bartholomeus et al., 2012; Witte et al., 2020b). Generally, extreme conditions were underestimated somewhat by the time series models. This overall underestimation of extreme conditions was also found by Mackay et al. (2015) with a process-based groundwater model. ~~An important shortcoming of the models is that they assume that the response time to recharge, or the lack of it, is constant for a given location. In reality, the response may be different during (extreme) drought conditions. This may contribute to less reliable TSM estimations during extreme groundwater drought.~~Interestingly, the simulations for summer 2018 showed an overestimation of drought conditions, where the simulations appeared to miss the variability towards less extreme drought that is visible in the measurements (Figs. 8, 9).

~~When considering the resulting drought index values, the time series models also appear to give a correct representation of overall drought dynamics.~~The model deviations during drought may be due to external influences not accounted for by the model, such as surface water influence and local irrigation, both of which are widespread in the study area. Indeed, local influences such as external water supply were found to alleviate groundwater drought locally in 2018 (Van den Eertwegh et al., 2019)~~The comparison of simulation- and measurement-based SGI values (Fig. 8) showed a good correlation (Spearman's~~

$\rho = 0.8$). The drought estimation is similar or slightly better than found by Van Loon et al. (2017), who simulated groundwater drought in the eastern Netherlands with a lagged SPEI-SGI correlation (Spearman's $\rho \approx 0.75$). Also, as discussed further below, the general patterns shown by the drought maps match well with the experience of water managers.

However, the comparison of simulation- and measurement-based SGI values also showed that the simulation-based drought quantification overestimated drought severity in the lowest ends of the 2018 drought, while also reducing the spatial variability. In summer and autumn 2018, the models simulated uniform extreme drought over the whole study area, while the measurement-based SGI values showed much more scatter towards less extreme drought (Fig. 8-9). It appears that the weather conditions were severe enough to trigger a 30-year extreme groundwater drought everywhere, but conditions not accounted for by the models, such as external water supply, caused the drought to be less extreme locally (Van den Eertwegh et al., 2019). In addition, the models may have underestimated the severity of earlier droughts; this would inflate the extremeness of the 2018 drought. Similar bias issues can be seen in Hellwig et al. (2020), who analysed groundwater drought in Germany using a physically-based model. Their simulations overestimated drought severity during a drought in 1973, but not in 2003, confirming that bias can differ between individual drought events. In their case, drought severities and bias therein were strongly influenced by the parameters related to the response time of the groundwater system. Similar issues may have played a role for the time series models used here.

Despite these shortcomings, the use of time series model simulations in drought analysis provides large advantages. In this study, it allowed for including a much larger number of series than if only long and disturbance-free series could have been used. This enabled a detailed image of drought development that would not have been possible by using direct measurement series only. In addition, the model parameters gave additional insight in groundwater behaviour, for example through the response time In addition, the deviations may be related to the model setup itself. As noted before, we have here worked with a simple linear recharge model. Although this has been shown to suffice in many situations (Bakker and Schaars, 2019; Collenteure.g. Zaadnoordijk et al., 2019; von Asmuth et al., 2012). Therefore, impulse-response time series simulations are considered a valuable tool for groundwater drought analysis in the Netherlands and other situations, although care must be taken for bias and (local) effects of non-weather influences on the groundwater system.

5.1.3 Potential of TSM for groundwater drought prediction

The findings also provide support for the usefulness of time series modelling for groundwater drought prediction. We found that, had perfect weather forecasts been available at the start of the growing season in 2018, the type of time series models used in this study would have reasonably predicted the course of the groundwater drought in summer and autumn, with an error of around 20 cm and low bias (Table 4). The potential for nowcasting, there are also various cases where linear recharge models were shown to be invalid (Bakker and Schaars, 2019; Collenteur et al., 2021). Nonlinear or threshold responses in the soil-groundwater system may be especially important during extreme conditions, as evapotranspiration and deep percolation may become limited by low soil moisture or drainage becomes disconnected (Bakker and Schaars, 2019; Aulenbach and Peters, 2018; Peterson and Western, 2014). Indeed, several studies have shown that nonlinear recharge representations can improve

Formatted: Font: Bold

model performance during (extreme) drought conditions (Berendrecht et al., 2006; Peterson and Western, 2014; Collenteur et al., 2021). The overestimation of drought severity in 2018 found here (Fig. 8) may, among other factors, be related to a lack of evapotranspiration limitation in the models (Collenteur et al., 2021). The effect of extreme drought on evapotranspiration and flowpaths can be complex and spatially variable (Teuling et al., 2013; Avanzi et al., 2020). Further exploring the value of nonlinear time series models for groundwater drought analyses in different situations is therefore an important topic for further research.

The reliability of groundwater simulations during extreme drought was found to be sensitive to the used calibration period, with reliability decreasing when the calibration period lacked similarly extreme conditions. This is an important aspect for the application of TSM for groundwater level nowcasting for real-time drought assessment. However, the difference in simulation performance compared to simulations that did include the 2018 drought in their calibration was relatively small (Table 5-6). This suggests that the type of impulse-response time series models used in this study are relatively robust for series lengthening and nowcasting, also in drought conditions. This is also shown by the lengthened series over 2019-2020, which matched well with general observations provided by other studies and reports (LCW, 2020; Van den Eertwegh et al., 2019). It was expected that the prediction of groundwater heads in periods of extreme drought would perform relatively poorly, as system conditions are being simulated that are not included in the calibration period. However, the errors of our predictions were close to those of the normal simulations that did include 2018 in their calibration (20 vs 18 cm, Table 3-4). The results also suggest that, over the time spans relevant for drought forecasting (months), updating forecasts with measurements may not be of much added value. This supports the idea that time series models, when based on sufficient calibration data, could be a relatively robust means for drought prediction over longer time spans.

Still, the prediction RMSE and mean errors amounted locally to high levels (Table 4). The drought index values in the main drought period of 2018 were predicted with an estimated error of 0.3 units, which can easily shift a location to a different drought category. The magnitude of these errors is similar to that reported by Marchant and Bloomfield (2018), who found that temporal interpolation of head measurement series with TSM led to an uncertainty in SGI values of roughly 0.1 to 0.2 in periods with good data cover, but much larger in longer periods with little data. In this study, we accounted only for the prediction error in drought severity resulting from model inaccuracy in the prediction period. In reality, the prediction uncertainty would obviously be increased by the uncertainty in the long-term weather forecasts (Honingh et al., 2020; Mackay et al., 2015).

Taken together, time series models show potential for groundwater drought nowcasting and forecasting on a general regional scale. HoweverStill, if water managers are to be provided structurally with up-to-date information on regional groundwater drought, theany models have to be re-calibrated with frequently, so that reliable, recent measurement data. Therefore, improving the accessibility and consistency of recent groundwater data among different organisations and countries remains an important task..

Formatted: Font: Not Bold

Despite the potential loss of information caused by TSM-based data preparation, consisting of processes and external influences not included in the models, it also provides important gains. Given the spatial variability in hydrological drought dynamics and the need for long data series for drought identification, TSM methods can be especially useful in drought studies to increase the amount of data available without a need for additional site information. In this study, it enabled a regional image of drought development (Figs. 5, 6) that is far more detailed than that obtained by using direct measurement series only (Fig. 9). In addition, the model parameters gave additional insight in groundwater behaviour, for example through the response time (Bakker and Schaars, 2019; Collenteur et al., 2019). TSM data preparation, especially if further developed, can therefore likely be useful in many regional groundwater drought studies. However, in some cases direct use of data, inclusion of more external drivers or (a combination with) more physically-based model methods will be more suitable (e.g. Bakker and Schaars, 2019) as in this study may have been the case for more local scales. The application of TSM methods therefore remains dependent on the aim and scale of a drought case study.

5.2 Analysis of the 2018-2019 groundwater drought in the Netherlands

5.2.1 Spatiotemporal development of groundwater drought in 2018-2019

The regional-scale analysis of the 2018-2019 groundwater drought in the southeastern Netherlands provided a new, detailed image of the drought development in time and space. The analysis showed that extreme groundwater drought was widespread over the study region in 2018 and 2019, breaking 30-year records for the summer and autumn months almost everywhere (Fig. 4). However, the timing and duration of the drought varied strongly in space. In the western parts of the study area drought was terminated before the end of 2018, while the higher-lying areas reached drought conditions only by 2019 (Fig. 5-6). This image corresponds well with how the drought was generally experienced by water managers. The Dutch Commission on Water allocation (LCW), which regularly surveys the drought status in the Netherlands based on input from water managers, reported widespread exceptional drops in groundwater levels, especially in the higher-lying sandy areas of the country, combined with a relatively fast recovery in the west (LCW, 2020). Also the severe damage observed in groundwater-dependent ecosystems in the southeastern Netherlands (Witte et al., 2020a) and widespread drying of groundwater-fed streams (Van den Eertwegh et al., 2019) match the assessment of an extreme groundwater situation.

The time series models made it possible to extend the available groundwater head measurement series beyond 2018 and obtain an estimate of drought recovery dynamics over 2019-2020. This showed that despite near-normal to high rainfall in the winters of 2018-19 and 2019-20 (Fig. 3) groundwater levels were restored only locally, and severe groundwater drought continued into 2019 or even 2020 over large parts of the study area (Fig. 6). These findings are consistent with general reports of the situation by local water managers (LCW, 2020; Van den Eertwegh et al., 2019). The results confirm that the drought should be viewed as a multi-year event rather than a single-year summer drought. The multi-year character increases the risk of lasting negative effects, especially in natural ecosystems. In addition, it stresses the importance of winter season groundwater management and water retention as determining factors in drought development. Both these issues have already become apparent in the Netherlands after 2018 (De Lenne and Worm, 2020; Witte et al., 2020a; Witte et al., 2020b).

5.2.2 Driving factors of spatial drought distribution

The current study did not aim to fully quantify the driving factors of the spatial variations in drought dynamics. However, the results suggest that the variation in drought severity, timing and duration was governed mainly by the spatial distribution in rainfall and the geological-topographic setting. The influence of spatial variations in weather was visible in late 2018 and 2019. In this period, a gradient in meteorological drought towards the east caused groundwater drought to be concentrated in this area. The effect of the geological-topographic setting is visible for the higher elevated parts of the study area, especially the glacial sand ridges and the limestone-loess hills, which clearly had a late, longlater, longer-lasting drought response compared tothan lower-lying areas (FigFigs. 5-6). This pattern is also visible in the groundwater response times (Fig. 7). The slow drought response in the higher elevated areas is likely explained by a thick unsaturated zone and low drainage density, while the fast recovery of the low-lying western parts may have been aided by thinner unsaturated zones and possibly some surface water influence. These factors have been found by other studies to influence drought behaviour (Bloomfield et al., 2015; Hellwig et al., 2020; Peters et al., 2006; Van Loon and Laaha, 2015; Kumar et al., 2016). In addition, the topographic-geological setting in the study area correlates with variations in land use, soil type and aquifer characteristics; these factors may have played an additional role.

The dominant role of landscape position in shaping drought development calls for locally adapted, but also regionally coordinated mitigation strategies. The response times obtained from the time series analysis form a useful first indicator of the landscape characteristics that control the propagation of meteorological drought to groundwater drought. The response times found here are somewhat shorter than the drought response times reported by Van Loon et al. (2017) for part of the eastern Netherlands. However, they are very similar to those found by Zaadnoordijk et al. (2019), who performed time series analysis on groundwater series from the whole Netherlands. As they used different data and different model quality criteria, the similarity is reassuring and points to the stability of the time series models.

6 Conclusions

The performed study aimed to evaluate the usefulness of time series modelling-based data processing methods for regional-scale groundwater drought monitoring and prediction.assessment. A TSM-based method was set up for data validation and drought quantification and applied to the regional 2018-2019 groundwater drought in the southeastern Netherlands to test its usefulness and reliability. It was found that the kind of groundwater data often available for drought studies requires a validation-cleaning step before analysis to enable reliable results. The validation method based on a combination of basic tests and time series modelling proved a suitable method for the given situation. StillAutomated TSM-based data validation was found able to improve the quality of input data. However, optimal validation parameters are likely to be context-dependent. In addition, improvements in the validation method are desired, especially in the separation of real and erroneous head disturbances. The simulated groundwater head series were generally found to be reliable; however, it was shown that the use of time series simulations may bias drought estimations and underestimate spatial variability, producing large errors at a local scale. Still, the use of time series model simulations in drought analysis provides large advantages, as it enables a spatially detailed record of drought development that may be impossible to obtain with direct measurement series only. ~~Time series models were also found to be a promising tool for regional-scale drought nowcasting and prediction, although the same caution for bias and local errors is needed.~~

The drought analysis for the southeastern Netherlands provided a complete, detailed image of the development of the 2018-2019 groundwater drought in time and space. The findings confirm that the meteorological drought in 2018 caused extreme groundwater drought throughout the southeastern Netherlands, starting in late spring and peaking in October-November of that year. The timing of drought onset and the duration of drought varied strongly in space. Drought development appeared to be governed dominantly by the spatial distribution of rainfall and the geological-topographic setting. In much of the area, the drought continued as a multi-year drought into 2019 and 2020, especially in the eastern and higher elevated regions.

Taken together, we conclude that time series modelling forms a useful tool to obtain a ~~quick~~fast, detailed and up-to-date image of drought development; however, for a proper understanding of the different driving factors of drought the availability of recent and consistent monitoring data remains crucial.

Appendix A

A1 Time series model setup

Groundwater head modelling was done by impulse-response transfer function-noise models using the Pastas package in Python (Python 3.6, Pastas 0.13). The model setup used in this study largely follows Collenteur et al. (2019). The code for building and simulating the models, as applied in the validation and simulation steps in this study, is given at the end of this section.

The working of impulse-response type transfer function-noise models for groundwater series is explained in von Asmuth (2002) and Collenteur et al. (2019). In principle, the method models groundwater heads as:

$$h(t) = \sum_{m=1}^{M} h_m(t) + d + r(t) \qquad \text{(A1)}$$

where h_m are the variations in heads caused by one or several stresses *m*; *d* is the base level; and *r* the residual at time *t*. Here only recharge was used as explanatory variable. Recharge is estimated as a linear combination of precipitation *P* and reference evapotranspiration ET_{ref}:

$$R(t) = P(t) - f \cdot ET_{ref} \qquad \text{(A2)}$$

With *f* a model parameter. The response of groundwater to a recharge impulse is calculated with a scaled gamma function (option *ps.Gamma* in Pastas):

$$\theta(t) = A \frac{t^{n-1}}{a^n \Gamma(n)} e^{-t/a} \qquad \text{(A3)}$$

With Γ the Gamma function, A a scale parameter and a and n shape parameters. The variation in groundwater heads over time h_m is obtained by convolution of this impulse-response function with the recharge time series.

This gives four parameters to be fit for each individual location. Parameter A represents the long-term response of the groundwater level to a constant recharge input of one unit, in this case 1 mm; f is the influence of ET_{ref} relative to precipitation; and d is the groundwater base level. For purposes of parameter calibration, also an AR(1) noise model is fit to the residuals, giving the additional noise decay parameter α. The default method for parameter optimisation was used, which minimises the sum of weighted squared noise by a least squares method (*ps.LeastSquares*). Table A1 gives the calibration settings for each of the parameters, as well as the range found in the raw groundwater head series in this study. Based on these ranges additional bounds were set for parameters A and f for the long-term behaviour classification (see section 3.2); series with unusual parameters beyond these bounds were classified as 'atypical' and potentially unreliable.

Formatted: Font: Italic

Table A1: Parameter calibration settings: initial value and bounds during optimisation (default settings Pastas); the range of values found in this study when modelling the initial 2723 cleaned series; and reliability bounds used for the series classification.

	Initial value (Pastas)	**Allowed range (Pastas)**	**Found values in this study (10^{th}-90^{th} percentile)**	**Reliability bounds for classification**
A	$1/\sigma_{recharge}$	≥0	0.10…1.2	≤1.5
a	10		72…473	
n	1		0.61…1.9	
f	-1	-2…0	-1.4…-0.44	-1.95…-0.05
d	Mean of series		0.95..41	
α	15		17…636	

Except for the simulations used to test the calibration period effect, the full period of available data between 1990 and 2019 was used for calibration. Calibration was done at a weekly timestep (recharge and observation series subsampled to a weekly frequency before optimisation) to allow a more even spread of optimisation points over time. Simulation of series was done at a daily timestep from 1990-01-01 to 2020-05-31.

```
"""
Basic time series model function for groundwater heads.
Based on Collenteur et al. (2019) doi: 10.1111/gwat.12925
Used in groundwater drought in the southern Netherlands project
Esther Brakkee, spring 2020
Applied with Pastas 0.13 and Python 3.6
"""
import pandas as pd
import Pastas as ps

def PastasModelParsSim (heads,rain,evap,calibstart="1990-01-01",
                        calibend="2019-12-31",simstart="1990-01-01",
                        simend="2020-05-31",method="Linear"):
    '''
    function to make a basic impulse-response time series model
    INPUT:
        -head dataframe with 'DateTime' in '%d-%m-%Y %H:%M' and 'Head' in m+MSL
       -daily-step series for rain and reference evapotranspiration, with
      'DateTime' in '%d-%m-%Y %H:%M' and 'Precip'/'Evap' in mm/d
    PARAMETERS:
        -calibstart, calibend: start and end of calibration period in
        '%Y-%m-%d'
       -simstart, simend: same for simulation period
       -ONLY LINEAR MODELLING FOR NOW
    OUTPUT:
        dictionary with simulated series, model parameters, fit criteria,
        residuals and noise
    '''
    #create model
    ml = ps.Model(heads, name='Model')
    if method=="Linear":
        rm = ps.RechargeModel(rain, evap, rfunc=ps.Gamma)#linear is default
    ml.add_stressmodel(rm)
    #solve model with weekly timestep
    ml.solve(freq="7D",tmin=calibstart,tmax=calibend,report=False)
    #get output
    res=ml.residuals()
    pars=ml.get_parameters() #A,n,a,f,d,noise-alpha
    evp=ml.stats.evp()
    noise=ml.noise()
    sim=ml.simulate(tmin=simstart, tmax=simend, freq="D")
    #all outcomes into a dictionary
    outcomes={"EVP":evp,"parameters":pars,"residuals":res,"method":method,
              "sim":sim,"noise":noise}
    return outcomes
```

A2 Validation parameter sensitivity

A2.1 Parameter sets

The validation routine was run with 21 different parameter sets (table A2). In set 2-11, the parameters are varied individually; in set 12-19, combinations of outlier cleaning and long-term deviation identification parameters are tested; and in set 20 and 21 versions are tested with only TSM-based outlier cleaning (no basic cleaning step) and no outlier cleaning at all.

Table A2: Used parameter sets for the sensitivity test. See table 1 for explanation of the parameters.

Nr	Name	Meta Check	F_{range}	TH_{red}	n_{SD}	n_{iter}	TH_{EVP}	TH_{r2}
1	*Standard*	*Yes*	*0.2*	*0.5*	*4*	*2*	*60*	*0.15*
2	FarOutliersConservative	Yes	0.1	0.7	4	2	60	0.15
3	FarOutliersRigorous	Yes	0.2	0.4	4	2	60	0.15
4	OutliersConservative	Yes	0.2	0.5	6	2	60	0.15
5	OutliersRigorous	Yes	0.2	0.5	2	2	60	0.15
6	IterationsConservative	Yes	0.2	0.5	4	1	60	0.15
7	IterationsRigorous	Yes	0.2	0.5	4	5	60	0.15
8	EVPConservative	Yes	0.2	0.5	4	2	40	0.15
9	EVPRigorous	Yes	0.2	0.5	4	2	80	0.15
10	TrendConservative	Yes	0.2	0.5	4	2	60	0.4
11	TrendRigorous	Yes	0.2	0.5	4	2	60	0.05
12	OutliersConservative_EVPConservative	Yes	0.1	0.7	6	1	40	0.15
13	OutliersConservative_EVPRigorous	Yes	0.1	0.7	6	1	80	0.15
14	OutliersConservative_TrendConservative	Yes	0.1	0.7	6	1	60	0.4
15	OutliersConservative_TrendRigorous	Yes	0.1	0.7	6	1	60	0.05
16	OutliersRigorous_EVPConservative	Yes	0.2	0.4	2	5	40	0.15
17	OutliersRigorous_EVPRigorous	Yes	0.2	0.4	2	5	80	0.15
18	OutliersRigorous_TrendConservative	Yes	0.2	0.4	2	5	60	0.4
19	OutliersRigorous_TrendRigorous	Yes	0.2	0.4	2	5	60	0.05
20	Standard_TSMcleaningOnly	No	0	1	4	2	60	0.15
21	Standard_NoOutlierCleaning	No	0	1	100	0	60	0.15

A2.2 Test results

Outliers

Table A3 gives the full outlier cleaning performance results for all parameter sets. Cleaning of outliers in general was able to increase the EVP of series TSM models from 60 % to 62 % on average (set 1 vs 21). Also, applying a cleaning step allows for more series to be retained. The basic, range-based outlier step adds relatively little to the cleaning quality compared to the time series model-based cleaning (set 20 vs 1). The range-based cleaning step appeared useful in a small number of cases where it improved the quality of the TSM cleaning; in addition, it is a computationally cheap step and was therefore retained in the validation.

As expected from the minor effect of the far outlier cleaning, the thresholds of this step have little effect on the validation performance (set 2 and 3). Changing the TSM-based outlier cleaning thresholds does result in large effects: lowering the SD threshold to 2·SD (set 5) causes the mean EVP (logically) to increase substantially, but also causes removal of many data points that would visually not be identified as errors (many false positives). Applying a more conservative TSM outlier cleaning with 6·SD (set 4) has the reverse effect, with many outliers not identified and more series being discarded. The number of iterations applied in the TSM outlier cleaning only slightly affected the resulting EVP of the series models. Apparently the first cycle already cleans the main outliers in most cases.

Table A3: Validation performance with regard to outliers. Left columns: number of series (of *n*=180) classified in each category. TP=outliers identified in manual and automatic validation; TN=outliers not identified in either manual or automatic validation; FP=outliers identified in automatic validation but not in manual validation; FN=outliers identified in manual but not in automated validation. Last column: percentage of series with outliers correctly cleaned.

Set	**Name**	**Missing Data**	**Outliers TP**	**Outliers TN**	**Outliers FP**	**Outliers FN**	**Mean EVP**	**Outliers Good [%]**
1	Standard	19	71	56	26	8	61.9	**79**
2	FarOutliersConservative	19	72	56	26	7	62	**80**
3	FarOutliersRigorous	19	71	56	26	8	61.9	**79**
4	OutliersConservative	19	36	92	5	28	60.6	**80**
5	OutliersRigorous	19	96	0	64	1	68.8	**60**
6	IterationsConservative	19	71	56	26	8	61.7	**79**
7	IterationsRigorous	19	71	56	26	8	62.2	**79**
8	EVPConservative	19	71	56	26	8	61.9	**79**
9	EVPRigorous	19	71	56	26	8	61.9	**79**
10	TrendConservative	19	71	56	26	8	61.9	**79**
11	TrendRigorous	19	71	56	26	8	61.9	**79**
12	OutliersConservative_ EVPConservative	19	37	92	5	27	60.5	**80**
13	OutliersConservative_ EVPRigorous	19	37	92	5	27	60.5	**80**
14	OutliersConservative_ TrendConservative	19	37	92	5	27	60.5	**80**
15	OutliersConservative_ TrendRigorous	19	37	92	5	27	60.5	**80**
16	OutliersRigorous_ EVPConservative	22	93	0	64	1	71.1	**59**
17	OutliersRigorous_ EVPRigorous	22	93	0	64	1	71.1	**59**
18	OutliersRigorous_ TrendConservative	22	93	0	64	1	71.1	**59**
19	OutliersRigorous_ TrendRigorous	22	93	0	64	1	71.1	**59**
20	Standard_ TSMcleaningOnly	19	73	54	26	8	62.1	**79**
21	Standard_ NoOutlierCleaning	19	0	110	0	51	59.9	**68**

Serious long-term deviations: discarding of series

Table A4 shows the validation performance with regard to serious long-term deviations in the series. Changing the EVP threshold for discarding series logically has a strong effect on the number of discarded series (set 8 and 9). Taking a conservative low EVP threshold appears to give a good performance on the strong deviation identification (set 8 and 16), but the number of false negatives, leading to potentially erroneous outcomes, is high. The outlier cleaning also affects the identification of long-term deviations. More rigorous outlier cleaning, especially by reducing the SD threshold, led to discarding a smaller number of series and slightly better performance on the long-term deviation identification, with conservative outlier cleaning having the reverse effect (set 2-5). However, the changes are small.

Table A4: Validation performance with regard to strong long-term deviation. Left columns: number of series (of *n*=180) classified in each category. TP=discarded in manual and automatic validation; TN=not discarded in either manual or automatic validation; FP=discarded in automatic validation but not in manual validation; FN=discarded in manual but not in automated validation. Excl deep: false positives excluding deep-GWL series. Discard number: number of series discarded of *n*=180. Last column: percentage of series with long-term strong deviation correctly identified.

Set	Name	Discard TP	Discard TN	Discard FP	Discard FP excl deep	Discard FN	Discard number	Discard Good [%]
1	Standard	32	103	26	22	0	58	**84**
2	FarOutliersConservative	32	103	26	22	0	58	**84**
3	FarOutliersRigorous	32	103	26	22	0	58	**84**
4	OutliersConservative	33	97	31	27	0	64	**81**
5	OutliersRigorous	24	115	17	13	5	41	**86**
6	IterationsConservative	32	100	29	25	0	61	**82**
7	IterationsRigorous	32	103	26	22	0	58	**84**
8	EVPConservative	17	121	12	8	11	29	**86**
9	EVPRigorous	34	42	85	73	0	119	**47**
10	TrendConservative	32	103	26	22	0	58	**84**
11	TrendRigorous	32	103	26	22	0	58	**84**
12	OutliersConservative_ EVPConservative	17	121	12	8	11	29	**86**
13	OutliersConservative_ EVPRigorous	34	39	88	74	0	122	**45**
14	OutliersConservative_ TrendConservative	33	95	33	29	0	66	**80**
15	OutliersConservative_ TrendRigorous	33	95	33	29	0	66	**80**
16	OutliersRigorous_ EVPConservative	12	129	3	1	14	15	**89**
17	OutliersRigorous_ EVPRigorous	32	76	50	41	0	82	**68**
18	OutliersRigorous_ TrendConservative	21	116	15	11	6	36	**87**
19	OutliersRigorous_ TrendRigorous	21	116	15	11	6	36	**87**
20	Standard_ TSMcleaningOnly	32	104	25	21	0	57	**84**

21	Standard_ NoOutlierCleaning	33	97	31	27	0	64	**81**

Mild long-term deviations: series to be marked as atypical

The fraction of series marked as atypical in the data is relatively small across the different parameter sets. The used r^2 threshold to identify trends affects this number. A high threshold of 0.4 results in very few atypical series being identified; a low threshold results in many false positives, as weak trends were present in a large proportion of the series. The identification of atypical series is also affected by the outliers cleaning parameters. More rigorous outlier cleaning (set 5) causes more series to be marked as atypical. Also the EVP threshold to discard series affects the number of series marked as atypical. With a high EVP threshold discards many mildly atypical series are discarded by an insufficient EVP. A low EVP threshold brings more series into the 'atypical' category.

Table A5: Validation performance with regard to mild long-term deviations. Left columns: number of series (of *n*=180) classified in each category. TP=marked as atypical in both manual and automatic validation; TN=not marked as atypical in either manual or automatic validation; FP=marked as atypical in automatic validation but not in manual validation; FN=marked as atypical in manual but not in automated validation. Excl deep: false positives excluding deep-GWL series. Atyp number: number of series marked atypical of n=180. Last columns: percentage of series with mild long-term deviations correctly identified.

Set	**Name**	**AtypTP**	**Atyp TN**	**Atyp FP**	**Atyp FP excl deep**	**Atyp FN**	**Atyp number**	**Atyp Good [%]**
1	Standard	7	131	11	7	12	18	86
2	FarOutliersConservative	7	131	11	7	12	18	86
3	FarOutliersRigorous	7	131	11	7	12	18	86
4	OutliersConservative	7	132	10	6	12	17	86
5	OutliersRigorous	9	123	19	14	10	28	82
6	IterationsConservative	7	131	11	7	12	18	86
7	IterationsRigorous	7	131	11	7	12	18	86
8	EVPConservative	10	119	23	18	9	33	80
9	EVPRigorous	0	142	4	2	15	4	88
10	TrendConservative	2	139	5	1	15	7	88
11	TrendRigorous	8	111	31	24	11	39	74
12	OutliersConservative_ EVPConservative	10	122	20	15	9	30	82
13	OutliersConservative_ EVPRigorous	0	142	4	2	15	4	88
14	OutliersConservative_ TrendConservative	2	139	5	1	15	7	88
15	OutliersConservative_ TrendRigorous	7	113	29	22	12	36	75
16	OutliersRigorous_ EVPConservative	13	106	32	24	7	45	75
17	OutliersRigorous_ EVPRigorous	2	135	6	4	15	8	87
18	OutliersRigorous_ TrendConservative	3	131	10	5	14	13	85

19	OutliersRigorous_ TrendRigorous	10	104	35	30	9	45	72
20	Standard_ TSMcleaningOnly	8	131	11	7	11	19	86
21	Standard_ NoOutlierCleaning	8	134	8	4	11	16	88

A3 Example figures

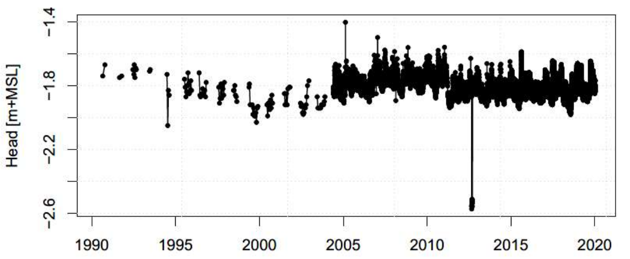

Figure A1: Example of a series with a clearly undesired outlier. The isolated low points in 2013 are caused by temporary extraction to clean the well. The series also contains smaller outliers in e.g. 1994 and 2006.

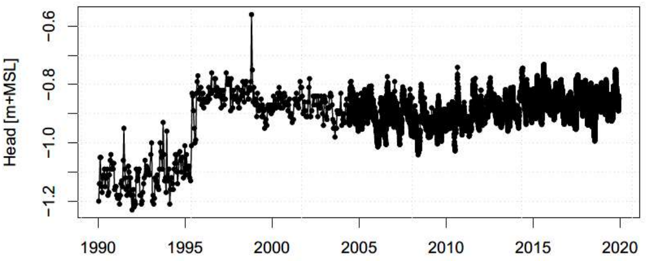

Figure A2: Example of a series with a serious long-term deviation. The level shift around 1996 is caused by changes in water management in the area. Also an outlier in 1999.

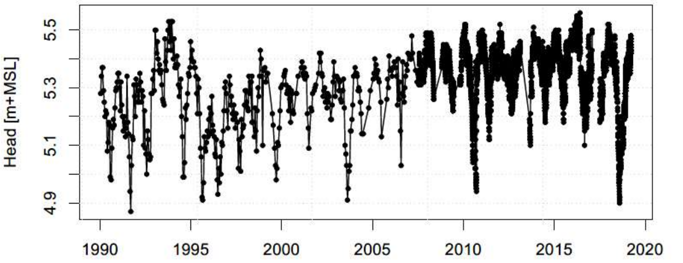

Figure A3: Example of a series with potentially unreliable long-term behaviour. There seems to be a trend from 1996 and a stabilisation after 2006, but the variations could be caused by weather variations and do not give reason to discard the series.

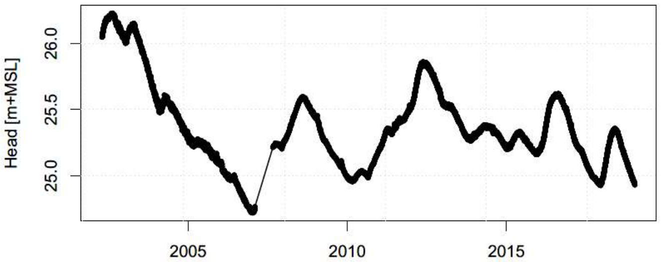

Figure A4: Example of a series with a deep groundwater table and resulting multi-year variation. Series located on the Veluwe ice-pushed ridge, mean WTD 35 m.

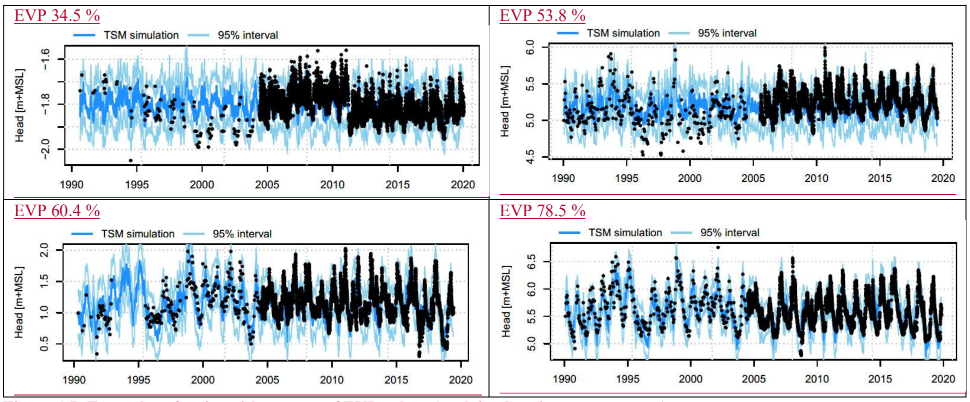

Figure A5: Examples of series with a range of EVP values (explained variance percentage).

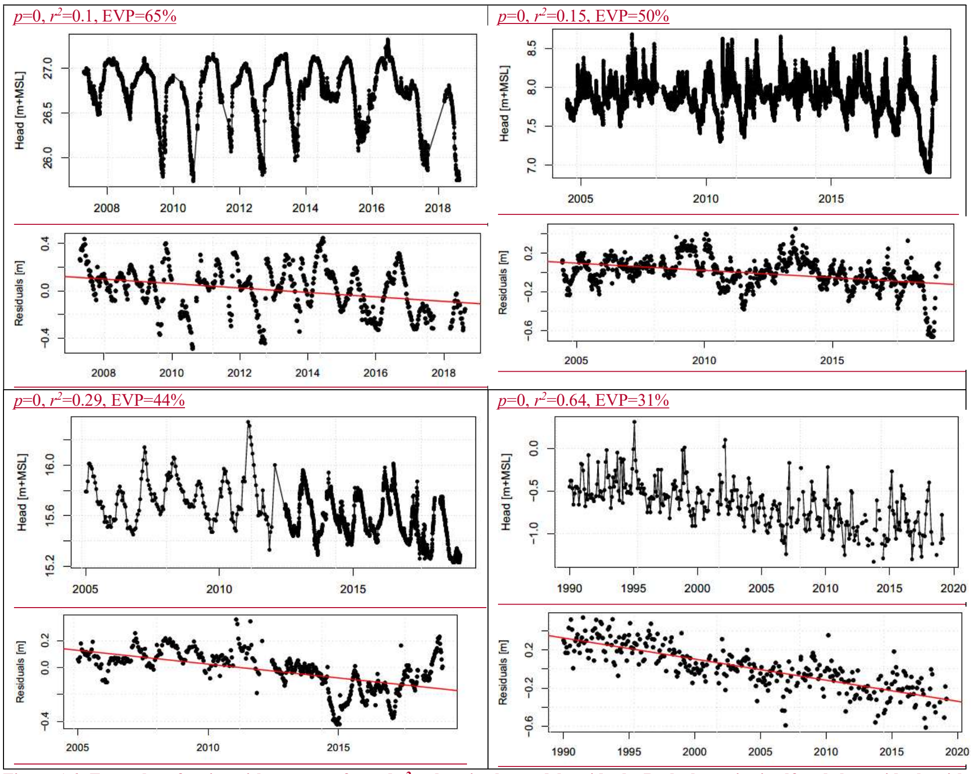

Figure A6: Examples of series with a range of trend r^2 values in the model residuals. Both the series itself and the residuals with fitted trend are shown.

Code and data availability

All code for data processing, modelling and visualisation is available on request from the first author. Groundwater data are freely available from the national groundwater database DINO (www.dinoloket.nl). The used weather data can be obtained from the Royal Dutch Meteorological Institute (KNMI) via http://projects.knmi.nl/klimatologie/daggegevens/selectie.cgi or through a script via https://www.knmi.nl/kennis-en-datacentrum/achtergrond/data-ophalen-vanuit-een-script.

Author contribution

EB, MvH and RB together designed the study. EB performed the study with advice from MvH and RB. The first article draft was written by EB and reviewed by all three authors.

Competing interests

The authors declare that they have no conflict of interest.

Acknowledgements

The authors thank Sharon Clevers for collecting and pre-processing an important part of the groundwater data.

References

AHN: AHN3 50cm maaiveld, Esri [Data set], https://www.arcgis.com/home/group.html?id=bd6fbbd182a9465ea269dd27ea985d1a#overview, 2019

Aulenbach, B. T., and Peters, N. E.: Quantifying Climate-Related Interactions in Shallow and Deep Storage and Evapotranspiration in a Forested, Seasonally Water-Limited Watershed in the Southeastern United States, Water Resources Research, 54, 3037-3061, https://doi.org/10.1002/2017WR020964, 2018.

Avanzi, F., Rungee, J., Maurer, T., Bales, R., Ma, Q., Glaser, S., and Conklin, M.: Climate elasticity of evapotranspiration shifts the water balance of Mediterranean climates during multi-year droughts, Hydrol. Earth Syst. Sci., 24, 4317-4337, 10.5194/hess-24-4317-2020, 2020.

Bakke, S. J., Ionita, M., and Tallaksen, L. M.: The 2018 northern European hydrological drought and its drivers in a historical perspective, Hydrol. Earth Syst. Sci., 24, 5621-5653, 10.5194/hess-24-5621-2020, 2020.

Bakker, M., and Schaars, F.: Solving Groundwater Flow Problems with Time Series Analysis: You May Not Even Need Another Model, Groundwater, 57, 826-833, https://doi.org/10.1111/gwat.12927, 2019.

Bartholomeus, R. P., Witte, J.-P. M., van Bodegom, P. M., and Aerts, R.: The need of data harmonization to derive robust empirical relationships between soil conditions and vegetation, Journal of Vegetation Science, 19, 799-808, https://doi.org/10.3170/2008-8-18450, 2008.

Bartholomeus, R. P., Witte, J.-P. M., van Bodegom, P. M., van Dam, J. C., de Becker, P., and Aerts, R.: Process-based proxy of oxygen stress surpasses indirect ones in predicting vegetation characteristics, Ecohydrology, 5, 746-758, https://doi.org/10.1002/eco.261, 2012.

Bastos, A., Ciais, P., Friedlingstein, P., Sitch, S., Pongratz, J., Fan, L., Wigneron, J. P., Weber, U., Reichstein, M., Fu, Z., Anthoni, P., Arneth, A., Haverd, V., Jain, A. K., Joetzjer, E., Knauer, J., Lienert, S., Loughran, T., McGuire, P. C., Tian, H., Viovy, N., and Zaehle, S.: Direct and seasonal legacy effects of the 2018 heat wave and drought on European ecosystem productivity, Science Advances, 6, eaba2724, 10.1126/sciadv.aba2724, 2020.

Berendrecht, W. L., Heemink, A. W., van Geer, F. C., and Gehrels, J. C.: A non-linear state space approach to model groundwater fluctuations, Advances in Water Resources, 29, 959-973, https://doi.org/10.1016/j.advwatres.2005.08.009, 2006.

Bloomfield, J. P., and Marchant, B. P.: Analysis of groundwater drought building on the standardised precipitation index approach, Hydrol. Earth Syst. Sci., 17, 4769-4787, 10.5194/hess-17-4769-2013, 2013.

Bloomfield, J. P., Marchant, B. P., Bricker, S. H., and Morgan, R. B.: Regional analysis of groundwater droughts using hydrograph classification, Hydrol. Earth Syst. Sci., 19, 4327-4344, 10.5194/hess-19-4327-2015, 2015.

Brauns, B., Cuba, D., Bloomfield, J. P., Brauns, B., Hannah, D. M., Jackson, C., Marchant, B., and . P., Heudorfer, B., Van Loon, A. F., Bessière, H., and Thunholm, B.: The Groundwater Drought Initiative (GDI): analysing and understanding groundwater drought across Europe EGU General Assembly, Vienna, Austria, 8-13 April 2018, 2018, Proceedings of the International Association of Hydrological Sciences, 383, 297-305, https://doi.org/10.5194/piahs-383-297-2020, 2020.

Brunner, M. I., Liechti, K., and Zappa, M.: Extremeness of recent drought events in Switzerland: dependence on variable and return period choice, Nat. Hazards Earth Syst. Sci., 19, 2311-2323, 10.5194/nhess-19-2311-2019, 2019.

Buras, A., Rammig, A., and Zang, C. S.: Quantifying impacts of the 2018 drought on European ecosystems in comparison to 2003, Biogeosciences, 17, 1655-1672, 10.5194/bg-17-1655-2020, 2020.

Collenteur, R. A., Bakker, M., Caljé, R., Klop, S. A., and Schaars, F.: Pastas: Open Source Software for the Analysis of Groundwater Time Series, Groundwater, 57, 877-885, https://doi.org/10.1111/gwat.12925, 2019.

Collenteur, R. A., Bakker, M., Klammler, G., and Birk, S.: Estimation of groundwater recharge from groundwater levels using nonlinear transfer function noise models and comparison to lysimeter data, Hydrol. Earth Syst. Sci., 25, 2931-2949, https://doi.org/10.5194/hess-25-2931-2021, 2021.

Dawley, S., Zhang, Y., Liu, X., Jiang, P., Tick, G. R., Sun, H., Zheng, C., and Chen, L.: Statistical analysis of extreme events in precipitation, stream discharge, and groundwater head fluctuation: Distribution, memory, and correlation, Water, 11, 707, https://doi.org/10.3390/w11040707, 2019.

De Lenne, R., and Worm, B.: Droogte 2018 & 2019: steppeachtige verschijnselen op de 'Hoge Zandgronden'. De gevolgen voor beheer en beleid bij Waterschap Vechtstromen, Stromingen, 25, 1-12, https://www.nhv.nu/wp-content/uploads/2020/06/2020-2_in_press_steppeachtige_verschijnselen_op_de_hoge_zandgronden.pdf, 2020.

Hellwig, J., de Graaf, I. E. M., Weiler, M., and Stahl, K.: Large-Scale Assessment of Delayed Groundwater Responses to Drought, Water Resources Research, 56, e2019WR025441, https://doi.org/10.1029/2019WR025441, 2020.

Honingh, D., Hurkmans, R., and Groot, S.: De toepasbaarheid van ECMWF-seizoensverwachtingen voor het voorspellen van grondwaterstanden, Stromingen, 2, https://www.nhv.nu/stroming/nieuws/de-toepasbaarheid-van-ecmwf-seizoensverwachtingen-voor-het-voorspellen-van-grondwaterstanden/, 2020.

IenW: Nederland beter weerbaar tegen droogte: Eindrapportage Beleidstafel Droogte, Ministerie van Infrastructuur en Waterstaat, https://www.rijksoverheid.nl/documenten/rapporten/2019/12/18/nederland-beter-weerbaar-tegen-droogte, 2019.

KNMI: Klimatologie/daggegevens, [Data set], https://www.knmi.nl/kennis-en-datacentrum/achtergrond/data-ophalen-vanuit-een-script, 2020

Kumar, R., Musuuza, J. L., Van Loon, A. F., Teuling, A. J., Barthel, R., Ten Broek, J., Mai, J., Samaniego, L., and Attinger, S.: Multiscale evaluation of the Standardized Precipitation Index as a groundwater drought indicator, Hydrol. Earth Syst. Sci., 20, 1117-1131, 10.5194/hess-20-1117-2016, 2016.

LCW: Archief droogtemonitoren 2018-2020, https://waterberichtgeving.rws.nl/LCW/droogtedossier/droogtemonitoren-archief/droogtemonitoren-2018, 2020.

Lehr, C., and Lischeid, G.: Efficient screening of groundwater head monitoring data for anthropogenic effects and measurement errors, Hydrol. Earth Syst. Sci., 24, 501-513, 10.5194/hess-24-501-2020, 2020.

Leunk, I.: Kwaliteitsborging grondwaterstands- en stijghoogtegegevens. Validatiepilot; analyse van bestaande data. , KWR Watercycle Research Institute, Nieuwegein, The Netherlands, 2014.059, https://edepot.wur.nl/317083, 2014.

Link, R., Wild, T. B., Snyder, A. C., Hejazi, M. I., and Vernon, C. R.: 100 years of data is not enough to establish reliable drought thresholds, Journal of Hydrology X, 7, 100052, https://doi.org/10.1016/j.hydroa.2020.100052, 2020.

Loáiciga, H. A.: Probability Distributions in Groundwater Hydrology: Methods and Applications, Journal of Hydrologic Engineering, 20, 04014063, 10.1061/(ASCE)HE.1943-5584.0001061, 2015.

Mackay, J. D., Jackson, C. R., Brookshaw, A., Scaife, A. A., Cook, J., and Ward, R. S.: Seasonal forecasting of groundwater levels in principal aquifers of the United Kingdom, Journal of Hydrology, 530, 815-828, https://doi.org/10.1016/j.jhydrol.2015.10.018, 2015.

Makkink, G.: Testing the Penman formula by means of lysimeters, Journal of the Institution of Water Engineers, 11, 277-288, 1957.

Marchant, B. P., and Bloomfield, J. P.: Spatio-temporal modelling of the status of groundwater droughts, Journal of Hydrology, 564, 397-413, https://doi.org/10.1016/j.jhydrol.2018.07.009, 2018.

Margariti, J., Rangecroft, S., Parry, S., Wendt, D. E., and Van Loon, A. F.: Anthropogenic activities alter drought termination, Elementa: Science of the Anthropocene, 7, 10.1525/elementa.365, 2019.

McKee, T. B., Doesken, N. J., and Kleist, J.: The relationship of drought frequency and duration to time scales, Proceedings of the 8th Conference on Applied Climatology, 1993, 179-183, 1993.

Peters, E., Bier, G., van Lanen, H. A. J., and Torfs, P. J. J. F.: Propagation and spatial distribution of drought in a groundwater catchment, Journal of Hydrology, 321, 257-275, https://doi.org/10.1016/j.jhydrol.2005.08.004, 2006.

Peterson, T. J., and Western, A. W.: Nonlinear time-series modeling of unconfined groundwater head, Water Resources Research, 50, 8330-8355, https://doi.org/10.1002/2013WR014800, 2014.

Peterson, T. J., Western, A. W., and Cheng, X.: The good, the bad and the outliers: automated detection of errors and outliers from groundwater hydrographs, Hydrogeology Journal, 26, 371-380, 10.1007/s10040-017-1660-7, 2018.

Pezij, M., Augustijn, D. C. M., Hendriks, D. M. D., and Hulscher, S. J. M. H.: The role of evidence-based information in regional operational water management in the Netherlands, Environmental Science & Policy, 93, 75-82, https://doi.org/10.1016/j.envsci.2018.12.025, 2019.

Philip, S. Y., Kew, S. F., van der Wiel, K., Wanders, N., and Jan van Oldenborgh, G.: Regional differentiation in climate change induced drought trends in the Netherlands, Environmental Research Letters, 15, 094081, 10.1088/1748-9326/ab97ca, 2020.

Post, V. E. A., and von Asmuth, J. R.: Review: Hydraulic head measurements—new technologies, classic pitfalls, Hydrogeology Journal, 21, 737-750, 10.1007/s10040-013-0969-0, 2013.

~~Sutanto, S. J., Wetterhall, F., and Van Lanen, H. A. J.: Hydrological drought forecasts outperform meteorological drought forecasts, Environmental Research Letters, 15, 084010, 10.1088/1748-9326/ab8b13, 2020.~~

Ritzema, H., Heuvelink, G., Heinen, M., Bogaart, P., van der Bolt, F., Hack-ten Broeke, M., Hoogland, T., Knotters, M., Massop, H., and Vroon, H.: Review of the methodologies used to derive groundwater characteristics for a specific area in The Netherlands, Geoderma regional, 14, e00182, 2018.

Svensson, C., Hannaford, J., and Prosdocimi, I.: Statistical distributions for monthly aggregations of precipitation and streamflow in drought indicator applications, Water Resources Research, 53, 999-1018, https://doi.org/10.1002/2016WR019276, 2017.

Teuling, A. J., Van Loon, A. F., Seneviratne, S. I., Lehner, I., Aubinet, M., Heinesch, B., Bernhofer, C., Grünwald, T., Prasse, H., and Spank, U.: Evapotranspiration amplifies European summer drought, Geophysical Research Letters, 40, 2071-2075, https://doi.org/10.1002/grl.50495, 2013.

TNO: DINOloket Ondergrondgegevens, Nederland, T. G. D. [Data set], https://www.dinoloket.nl/ondergrondgegevens,

Toreti, A., Belward, A., Perez-Dominguez, I., Naumann, G., Luterbacher, J., Cronie, O., Seguini, L., Manfron, G., Lopez-Lozano, R., Baruth, B., van den Berg, M., Dentener, F., Ceglar, A., Chatzopoulos, T., and Zampieri, M.: The Exceptional 2018 European Water Seesaw Calls for Action on Adaptation, Earth's Future, 7, 652-663, https://doi.org/10.1029/2019EF001170, 2019.

Van de Velde, I., van der Kooij, S., Van Hussen, K., and Läkamp, R.: Economische schade door droogte in 2018, Ecorys, Rotterdam, the Netherlands, https://www.rijksoverheid.nl/documenten/rapporten/2019/08/31/economische-schade-door-droogte-in-2018, 2019.

Van den Eertwegh, G., Bartholomeus, R., De Louw, P., Witte, F., van Dam, J., Van Deijl, D., Hoefsloot, P., Sharon, C., Van Huijgevoort, M., Hunink, J., Mulder, N., Pouwels, J., and De Wit, J.: Droogte in zandgebieden van Zuid-, Midden- en Oost-Nederland: Rapportage fase 1: ontwikkeling van uniforme werkwijze voor analyse van droogte en tussentijdse bevindingen., KnowH2O, https://edepot.wur.nl/511196, 2019.

Van Loon, A. F.: Hydrological drought explained, WIREs Water, 2, 359-392, https://doi.org/10.1002/wat2.1085, 2015.

Van Loon, A. F., and Laaha, G.: Hydrological drought severity explained by climate and catchment characteristics, Journal of Hydrology, 526, 3-14, https://doi.org/10.1016/j.jhydrol.2014.10.059, 2015.

Van Loon, A. F., Stahl, K., Di Baldassarre, G., Clark, J., Rangecroft, S., Wanders, N., Gleeson, T., Van Dijk, A. I. J. M., Tallaksen, L. M., Hannaford, J., Uijlenhoet, R., Teuling, A. J., Hannah, D. M., Sheffield, J., Svoboda, M., Verbeiren, B., Wagener, T., and Van Lanen, H. A. J.: Drought in a human-modified world: reframing drought definitions, understanding, and analysis approaches, Hydrol. Earth Syst. Sci., 20, 3631-3650, 10.5194/hess-20-3631-2016, 2016.

Van Loon, A. F., Kumar, R., and Mishra, V.: Testing the use of standardised indices and GRACE satellite data to estimate the European 2015 groundwater drought in near-real time, Hydrol. Earth Syst. Sci., 21, 1947-1971, 10.5194/hess-21-1947-2017, 2017.

Vicente-Serrano, S. M., Beguería, S., and López-Moreno, J. I.: A Multiscalar Drought Index Sensitive to Global Warming: The Standardized Precipitation Evapotranspiration Index, Journal of Climate, 23, 1696-1718, 10.1175/2009JCLI2909.1, 2010.

von Asmuth, J. R., Bierkens, M. F. P., and Maas, K.: Transfer function-noise modeling in continuous time using predefined impulse response functions, Water Resources Research, 38, 23-21-23-12, https://doi.org/10.1029/2001WR001136, 2002.

von Asmuth, J. R., Maas, K., Knotters, M., Bierkens, M. F. P., Bakker, M., Olsthoorn, T. N., Cirkel, D. G., Leunk, I., Schaars, F., and von Asmuth, D. C.: Software for hydrogeologic time series analysis, interfacing data with physical insight, Environmental Modelling & Software, 38, 178-190, https://doi.org/10.1016/j.envsoft.2012.06.003, 2012.

~~Wanders, N., Thober, S., Kumar, R., Pan, M., Sheffield, J., Samaniego, L., and Wood, E. F.: Development and Evaluation of a Pan-European Multimodel Seasonal Hydrological Forecasting System, Journal of Hydrometeorology, 20, 99-115, 10.1175/JHM-D-18-0040.1, 2019.~~

Witte, F., Runhaar, J., and van den Eertwegh, G.: Verdroging van de Nederlandse natuur: bijna een halve eeuw goed onderzoek en falende politiek., Stromingen, 26, 65-80, https://www.nhv.nu/stroming/nieuws/verdroging-van-de-nederlandse-natuur-bijna-een-halve-eeuw-goed-onderzoek-en-falende-politiek/, 2020a.

Witte, F., van Deijl, D., and van den Eertwegh, G.: Gevolgen voor de natuur op de hogere zandgronden van de droge jaren 2018 en 2019; Resultaten van een enquête onder deskundigen., FWE, KnowH2O, https://edepot.wur.nl/521008, 2020b.

WUR: Grondsoortenkaart 2006, Research, W. U. [Data set], https://www.wur.nl/en/show/Grondsoortenkaart.htm, 2006

Zaadnoordijk, W. J., Bus, S. A. R., Lourens, A., and Berendrecht, W. L.: Automated Time Series Modeling for Piezometers in the National Database of the Netherlands, Groundwater, 57, 834-843, https://doi.org/10.1111/gwat.12819, 2019.

Page 16: [1] Merged Cells	Brakkee, Esther	1-10-2021 10:02:00

Merged Cells

Page 16: [2] Formatted	Brakkee, Esther	1-10-2021 10:02:00

Font: +Body (Times New Roman), 9 pt, Bold

Page 16: [3] Formatted	Brakkee, Esther	1-10-2021 10:02:00

Left, Line spacing: single

Page 16: [4] Formatted Table	Brakkee, Esther	1-10-2021 10:02:00

Formatted Table

Page 16: [5] Formatted	Brakkee, Esther	1-10-2021 10:02:00

Font: +Body (Times New Roman), 9 pt, Bold

Page 16: [6] Formatted	Brakkee, Esther	1-10-2021 10:02:00

Font: +Body (Times New Roman), 9 pt, Bold

Page 16: [7] Inserted Cells	Brakkee, Esther	1-10-2021 10:02:00

Inserted Cells

Page 16: [8] Inserted Cells	Brakkee, Esther	1-10-2021 10:02:00

Inserted Cells

Page 16: [9] Inserted Cells	Brakkee, Esther	1-10-2021 10:02:00

Inserted Cells

Page 16: [10] Inserted Cells	Brakkee, Esther	1-10-2021 10:02:00

Inserted Cells

Page 16: [11] Formatted	Brakkee, Esther	1-10-2021 10:02:00

Left, Line spacing: single

Page 16: [12] Formatted	Brakkee, Esther	1-10-2021 10:02:00

Font: +Body (Times New Roman), 9 pt, English (United Kingdom)

Page 16: [13] Formatted	Brakkee, Esther	1-10-2021 10:02:00

Font: +Body (Times New Roman), 9 pt, English (United Kingdom)

Page 16: [14] Formatted	Brakkee, Esther	1-10-2021 10:02:00

Font: +Body (Times New Roman), 9 pt, English (United Kingdom)

Page 16: [15] Formatted	Brakkee, Esther	1-10-2021 10:02:00

Font: +Body (Times New Roman), 9 pt, English (United Kingdom)

Page 16: [16] Formatted	Brakkee, Esther	1-10-2021 10:02:00

Font: +Body (Times New Roman), 9 pt, English (United Kingdom)

Page 16: [17] Formatted	Brakkee, Esther	1-10-2021 10:02:00

Font: +Body (Times New Roman), 9 pt, English (United Kingdom)

Page 16: [18] Formatted	Brakkee, Esther	1-10-2021 10:02:00

Left, Line spacing: single

Page 16: [19] Formatted **Brakkee, Esther** **1-10-2021 10:02:00**

Font: +Body (Times New Roman), 9 pt, Bold, English (United Kingdom)

Page 16: [20] Formatted **Brakkee, Esther** **1-10-2021 10:02:00**

Font: +Body (Times New Roman), 9 pt, Bold, English (United Kingdom)

Page 16: [21] Formatted **Brakkee, Esther** **1-10-2021 10:02:00**

Font: +Body (Times New Roman), 9 pt, Bold, English (United Kingdom)

Page 16: [22] Formatted **Brakkee, Esther** **1-10-2021 10:02:00**

Font: +Body (Times New Roman), 9 pt, Bold

Page 16: [23] Formatted **Brakkee, Esther** **1-10-2021 10:02:00**

Font: +Body (Times New Roman), 9 pt, Bold

Page 16: [24] Formatted **Brakkee, Esther** **1-10-2021 10:02:00**

Font: +Body (Times New Roman), 9 pt, Bold, English (United Kingdom)

Page 16: [25] Formatted **Brakkee, Esther** **1-10-2021 10:02:00**

Left, Line spacing: single

Page 16: [26] Formatted **Brakkee, Esther** **1-10-2021 10:02:00**

Font: +Body (Times New Roman), 9 pt, English (United Kingdom)

Page 16: [27] Formatted **Brakkee, Esther** **1-10-2021 10:02:00**

Font: +Body (Times New Roman), 9 pt, English (United Kingdom)

Page 16: [28] Formatted **Brakkee, Esther** **1-10-2021 10:02:00**

Font: +Body (Times New Roman), 9 pt, English (United Kingdom)

Page 16: [29] Formatted **Brakkee, Esther** **1-10-2021 10:02:00**

Font: +Body (Times New Roman), 9 pt, English (United Kingdom)

Page 16: [30] Formatted **Brakkee, Esther** **1-10-2021 10:02:00**

Font: +Body (Times New Roman), 9 pt, English (United Kingdom)

Page 16: [31] Formatted **Brakkee, Esther** **1-10-2021 10:02:00**

Font: +Body (Times New Roman), 9 pt, English (United Kingdom)

Page 16: [32] Formatted **Brakkee, Esther** **1-10-2021 10:02:00**

Left, Line spacing: single

Page 16: [33] Formatted **Brakkee, Esther** **1-10-2021 10:02:00**

Font: +Body (Times New Roman), 9 pt, Bold, English (United Kingdom)

Page 16: [34] Formatted **Brakkee, Esther** **1-10-2021 10:02:00**

Font: +Body (Times New Roman), 9 pt, Bold, English (United Kingdom)

Page 16: [35] Formatted **Brakkee, Esther** **1-10-2021 10:02:00**

Font: +Body (Times New Roman), 9 pt, Bold, English (United Kingdom)

Page 16: [36] Formatted	Brakkee, Esther	1-10-2021 10:02:00

Font: +Body (Times New Roman), 9 pt, Bold, English (United Kingdom)

Page 16: [37] Formatted	Brakkee, Esther	1-10-2021 10:02:00

Font: +Body (Times New Roman), 9 pt, Bold

Page 16: [38] Formatted	Brakkee, Esther	1-10-2021 10:02:00

Font: +Body (Times New Roman), 9 pt, Bold

Page 16: [39] Formatted	Brakkee, Esther	1-10-2021 10:02:00

Left, Line spacing: single

Page 16: [40] Formatted	Brakkee, Esther	1-10-2021 10:02:00

Font: +Body (Times New Roman), 9 pt

Page 16: [41] Formatted	Brakkee, Esther	1-10-2021 10:02:00

Font: +Body (Times New Roman), 9 pt

Page 16: [42] Formatted	Brakkee, Esther	1-10-2021 10:02:00

Font: +Body (Times New Roman), 9 pt

Page 16: [43] Formatted	Brakkee, Esther	1-10-2021 10:02:00

Font: +Body (Times New Roman), 9 pt

Page 16: [44] Formatted	Brakkee, Esther	1-10-2021 10:02:00

Font: +Body (Times New Roman), 9 pt

Page 16: [45] Formatted	Brakkee, Esther	1-10-2021 10:02:00

Font: +Body (Times New Roman), 9 pt

Page 16: [45] Formatted	Brakkee, Esther	1-10-2021 10:02:00

Font: +Body (Times New Roman), 9 pt

Page 16: [46] Formatted	Brakkee, Esther	1-10-2021 10:02:00

Font color: Accent 1, English (United Kingdom)